FACULTY OF ENGINEERING AND ARCHITECTURE

Evaluating the human exposure of a UAV-aided network

Thomas Detemmerman
Student number: 01707806

Supervisors: Prof. dr. ir. Wout Joseph, Prof. dr. ir. Luc Martens
Counsellors: Dr. ir. Margot Deruyck, German Dario Castellanos Tache

Master's dissertation submitted in order to obtain the academic degree of
Master of Science in Information Engineering Technology

Academic year 2019-2020

GHENT UNIVERSITY

Dankwoord

todo

Contents

List of Figures

List of Tables

List of Listings

Glossary

equivalent isotropic radiator A theoretical source of electromagnetic waves which radiates the same intensity for all directions.. 21, 22, 39, 46

RRP RRP is an abreviation used in this paper to indicate an extension on EIRP and stands for Real Radiation Pattern. An RRP value indicates the power (in dBm) for a certain location unlike an EIRP where the power (in dBm) is independent of the location.. 25

spurious radiation according to the thefreedictionary.com: Any emission from a radio transmitter at frequencies outside its frequency band. Also known as spurious emission.. 17

Acronyms

DL downlink. 15, 16, 26, 41, 46

EIRP Equivalent Isotropical Radiation Power. 20, 25, 41, 42

FDD frequency division duplex. 16

ICNIRP International Commission on Non-Ionizing Radiation Protection. 13, 14

IEC International Electrotechnical Commission. 27

LTE Long-Term Evolution. 16, 20, 39, 40

SAR Specific Absorption Rate. 14, 23

TDD time division duplex. 16

UABS Unmanned Arial Base Station. 10, 12, 13, 15, 19–21, 24, 26, 28, 32, 33, 35, 36, 38–43, 46

UE User Equipment. 13, 19–21, 24, 26, 27, 41, 46

UL uplink. 14–16, 24, 26, 27, 41, 46

1

Introduction

1.1 Outline of the issue

Society is constantly getting more and more dependent on wireless communication. On any given moment, in any given location, an electronic device can request to connect to the bigger network. Devices need more then ever to be connected, starting from small IOT sensors up to self-driving cars which all need to be supported by the existing infrastructure. Once again it becomes clear why we're on the eve of a new generation of cellular communication named 5G. This new technology is capable of handling millions of connections every square meter while satisfying only a few microseconds of a delay and providing connections up to 10Gbps [1].

Also in exceptional and possibly life-threatening situations, the public relies on the cellular network. For example during the terrorist attacks in Zaventem, a Belgian city, mobile network operators saw all telecommunications drastically increasing causing moments of contention. Some operators decided to temporarily exceed the exposure limits in order to handle all connections. [2]

Electromagnetic exposure can however not be neglected. Research shows how excessive electromagnetic radiation can cause diverse biological side effects [3]. Because of public concern, the World Health Organization had launched a large, multidisciplinary research effort which

eventually concluded that there was no sufficient evidence that confirmed that exposure to low level electromagnetic fields is harmful [4]. A large part of the population remains nevertheless very concerned about potential health risks.

1.2 Objective

It becomes clear that electromagnetic exposure is an important asset when designing a network. This master dissertation will investigate the electromagnetic exposure of the citizen of Ghent which has a 97% coverage of 4G on average over all telecom operators[5].

People are constantly getting exposed to several sources of electromagnetic radiation. For this research, three prominent sources of radiation in a telecommunication network are investigated, being: the user his own phone, all base stations and all devices from other users in the network. In order to calculate electromagnetic exposure from all these sources, various parameters need to be known. Not only the used technology but also the position of the users and base stations need to be known. There are several publications discussing how the electromagnetic exposure originating from base stations can be calculated. Papers who cover electromagnetic exposure from all these different sources and convert it into a single value are rather limited.

To make this research possible, an existing planning tool is used which gives insight in user and base station distributions. The tool also provides information about pathloss between radiators, power usage of the different electrical devices and which base stations handle which users. The tool describes in other words a fully configured network. In this way, all needed parameters will be known.

The electromagnetic behavior of the network will be analysed by applying the tool in different scenarios to give insight which variables influence the exposure and how the network can be optimized accordingly.

research question 1: How can a Unmanned Arial Base Station (UABS) network be optimized to minimize global exposure and overall power consumption? What are the effects on the network?

research question 2: What are the advantages and disadvantages of a model as described in research question 1 compared the the already existing pathloss oriented model.

research question 3: How does the UABS fly height influence uplink and downlink exposure?

1.3 Structure

TODO: update this section

2

State of the art

2.1 Deployment tool for an UAV network

Calculating electromagnetic exposure requires knowledge about the area. The position of base stations need to be known, the transmission power used by the antenna and how far the user is separated from this base stations are only a few parameters that have to be considered.

The WAVES research group at UGent has developed a deployment tool for disaster scenarios with the aid of UAVs [6]. The idea of this UAV-aided emergency network is that in case of a disaster, the existing network might be damaged and won't be able to handle all users who are trying to reconnect to the backbone network. The tool makes a fast deployable network possible by attaching femtocells to UAVs, so-called UABSs. The tool will orchestrate the UABSs over the disaster area. This tool is thus a suitable starting point and works as follows:

The deployment tool will try to calculate the optimal placement for each UABS and requires therefore a description of the area where the UAV-aided network needs to be deployed. This is done with the use of so-called shape files. These files contain three dimensional descriptions of the buildings present in the area and are key values in approaching results as realistic as possible. Furthermore, the tool also requires a time period and a configuration file containing technical specifications of the type of UABS that is being used. The tool will thereafter ran-

domly distribute users over the area and assigns a certain bitrate to them.

In a second phase, the optimal position for each UABS is calculated. This is done by trying to locate a UABS above each active user. Two options are possible. If a flying height is defined, a base stations is placed above each user at the given height, unless a building is obstructing it's location. Then, no base station will be located above that user. If no flying height is given to the tool, the base station is located 4 meters above the outdoor user or 4 meters above the building where the indoor user resides. The latter is only allowed if the suggested height remains below the given maximum allowed height.

Finally, all UABS are sorted on wether they were active or not, followed by the increasing pathloss from each UABS to that user. So the algorithm starts by checking for each active UABS if it can cover the user. If this is the case, the user will be connected to this UABS. If not, the second active base station with a (slightly) worse pathloss is considered. If no active base station is suitable, inactive UABS are considered. The user remains uncovered if no UABS is found. The reason behind first only considering base stations that are already active, is the hight cost that comes along with each drone.

Up till now, the tool has only calculated some suggestions. The effective provisioning is done in the fourth phase where drones are sorted by the amount of users it cover. As long as UABS are available in the facility where they reside, UABS are provisioned and its users are marked as covered.

2.2 Electromagnetic exposure

2.2.1 Electromagnetic field radiation

People in a telecommunication network are exposed to far field electromagnetic radiation originating from base stations and other User Equipment (UE). Network planners need to make sure that the electromagnetic fields (expressed in V/m) do not exceed limitations enforced by the government. These limits are location dependent. The European Union recommend the guidelines as defined by the International Commission on Non-Ionizing Radiation Protection (ICNIRP) which limits electromagnetic exposure to 61 V/m. Each european country needs to decide for themselves which limitations to enforce. Belgium for example delegated this responsibility to Flanders, Brussels and Wallonia [7].

The used deployment tool is applied in Ghent, a Flemish city in Belgium. The standards defined by the Flemish government are therefore applicable. They state that in the 2.6 Ghz frequency

band, an individual antenna can't exceed 4.5 V/m and the cumulative sum of all fixed sources 31 V/m [8].

2.2.2 Specific Absorption Rate

Specific Absorption Rate (SAR) represents the rate that electromagnetic energy is absorbed by human tissue with the thermal effect as it's most important health consequence. The volume of this tissue is typically 1g or 10g. The Federal Communications Commission of the United States defines regulations based on 1g tissue (indicated as SAR_{1g}) while the European Union handles the 10g model (SAR_{10g}). SAR values can further be categorized based on the area it covers. A first one is whole body SAR (SAR^{wb}) which is the average absorbed radiation over the entire body. The second type is more precisely. Localized SAR-values cover only a part of the human body like the head. The ICNIRP has concluded that the threshold effect for SAR^{wb}_{10g} is at 4 W/kg meaning that any higher absorption rate would overwhelm the thermoregulatoy capacity of the human body. Whole body values between 1 and 4 W/kg increase the temperature of human body less than 1°C, which is proven not to be harmful for a healthy human being[9]. Thereafter, a safety margin is introduced to tackle unknown variables like experimental errors, increased sensitivity for certain population groups and so on. This results in a whole body SAR_{10g} of $0.8W/kg$ and $2W/kg$ for localized SAR_{10g} at head and torso area [7].

2.2.3 Related work

The goals of this master dissertation is the investigation of electromagnetic exposure considering all sources. Three types of sources are considered: electromagnetic radiation caused by basestations, near field radiation from the users own device and far field radiation originating from other users their equipment. This electromagnetic radiation is thereafter absorbed by the human body which will be expressed in SAR values.

Several papers exist calculating exposure originating from certain sources, but very limited research has been done covering the whole picture. In [10] is described how electromagnetic radiation of several WiFi access points is being calculated. The authors of [11] used this knowledge to investigate electromagnetic exposure originating from basestations in a more outdoor environment. [12, 13] addresses the fact that also uplink (UL) traffic from the user's device should be considered. They therefore investigated indoor exposure. They did not only consider the electromagnetic radiation but also how much is absorbed by the body which will be expressed as specific absorption rate. Since the authors only covered voice calls, uplink SAR was expressed in localized SAR values while the downlink traffic is expressed in whole body SAR. With the advent of 5G, paper [14] has been published describing how localized SAR values are

achieved from all sources. More precisely: all mobile phones and all basestations in the network after which they converted the electromagnetic exposure to localized SAR values. Finally, [15] describes how both UL and downlink (DL) traffic can be converted in whole body SAR values making it possible to achieve an overall picture. They applied this formula however only for the user's own device.

In a realistic network like the used deployment tool, some users are calling while another part is using other types of telecommunication services like browsing the web. Therefore, all absorbed electromagnetic exposure should be expressed in whole body SAR while still covering all sources.

2.3 Optimizing towards electromagnetic exposure and power consumption

UABSs are drones with femtocell base stations attached to it. Drones can remain in the air for only a limited time, which is certainly the case when also an antenna needs to be connected to the battery of his carrier. It is therefore interesting to not only consider electromagnetic exposure of the user but also the power consumption that comes with it. However an increasing transmission power of an antenna comes with an increasing electromagnetic exposure. This is not the case considering both values for an entire network. In fact, the autors from [11] prove that both become inversely equivalent.

If a network is optimized towards power consumption, less drones will be provisioned radiating at higher power levels. This is because not only the transmission power is considered but also the power needed to keep the drone in the air. Therefore, it is cheaper to cover a user by increasing the antennae transmission power of an already activated drone nearby as it therefore prevents the power cost of a new drone. By increasing the transmission power, also the electomagnetic exposure will increase for users closer to that drone. An exposure optimized network will therefore faster decide to power up a new drone.

todo: geen grid maar per user–> methodology

2.4 Technologies

2.4.1 Type of drone

Section 2.1 describes how femtocell antennae will be connected to helicopter drones. Two types of drones are considered in [6]: an off-the-shelf drone affordable by the general public and a

more expensive drone. The results in [6] show that the second type will require less drones to cover the same number of users and will last longer in the air. The research in this paper will therefore be done with the usage of the second type. A technical overview of this drone is given in table 2.1.

Parameter	value
Carrier power	13.0 A
Average carrier speed	12.0 m/s
Average carrier power usage	17.33 Ah
Carrier battery voltage	22.2 V

Table 2.1: specifications for the used drone.

2.4.2 LTE

The tool makes usage of Long-Term Evolution (LTE) which is by the general public better known as 4G which allows better UL and DL data speeds compared to its predecessors and is based on an all IP architecture. LTE can cover macrocells supporting cell sizes ranging from 5 km up to 100 km. These types of antennae are usually attached to transmission towers along highways or on top of buildings. LTE supports however also smaller cells like femtocells covering only a few hundred meters. They are therefore more portable, require less energy and won't require a telecommunication operator because of their simplicity. Femtocell base stations are therefore used by the deployment tool. Further, LTE also support both frequency division duplex (FDD) and time division duplex (TDD).

FDD makes simultaneous UL and DL traffic possible by assigning different frequencies within the frequency range to both data streams. A small guard band is used between UL and DL directions in other to prevent interference.

TDD allows UL and DL by splitting the time domain. Meaning that both traffic directions use the same frequency and therefore alternately (in time) use the frequency spectrum. A small time interval is used to prevent interference in case of a slightly bad timed synchronization.

This master dissertation will make usage of FDD.

2.4.3 Type of antenna

An important part of this master dissertation is the type of antenna that will be used by the femtocell base stations. The deployment tool makes use of drones that will position the femtocell base stations in the right position. Using conventional sector antennae, as used by traditional

terrestrial transmission towers, would be to complicated for a simple drone. The characteristics of microstrip antennae will therefore be investigated.

Microstrip antennae provide several advantages compared to traditional antennae [16, 17]. Microstrip antennae are lightweight, low in cost and thin causing them to be more aerodynamic which is a useful feature since the antennae will be attached to flying drones.

A basic microstrip antenna like figure 2.1 consists out of a ground plane and a radiating patch, both separated with a dielectric substrate. Several variations exist like microstrip patch antenna, microstrip slot antenna and printed dipole antenna which all have similar characteristics. They are all thin, support dual frequency operation and they all have the disadvantage that they will transmit at frequencies outside the aimed band which is also known as spurious radiation. The microstrip patch and slot antenna support both linear and circular polarization while the printed dipole only supports linear polarization. Further is the fabrication of a microstrip patch antenna considered to be the easiest of its competitors.

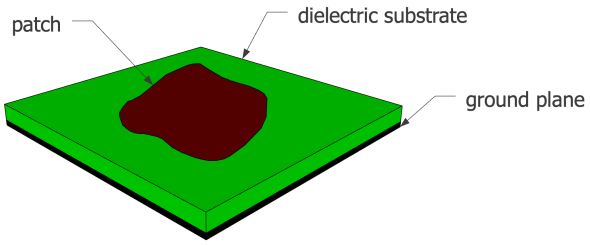

Figure 2.1: General design of a microstrip antenna

The microstrip antenna requires besides the groundplane, dielectric substrate and the radiation patch also a feed line. Several feeding techniques exist of which the most popular are: coaxial probe feeding, microstrip line and aperture coupling. (todo: more refs? gebruik nummer twee van J13 (p2))

A first feeding method is with the usage of a coaxial cable where the outer conductor is attached to the ground plane and the inner conductor to the radiations patch. Modelling is however difficult, especially for thick substrates as will be used in this master dissertation. A second option is the usage of a microstrip line. This type of feeding is much easier to model since the microstrip line can be seen as en extension of the radiating patch. A disadvantage is the increased spurious radiation which limits bandwith. A third is proximity coupling which has the largest bandwidth and low spurious radiation. It consist however of two dielectric substrates causing the overall thickness of the antenna to increase as well as it's fabrication difficulty. (todo: tekst te weinig, bespreek ook apperture coupled attenna (zelfde paper als de rest))

The increasing usage of the microstrip patch antennae can be explained by it's easy fabrication

and lightweightness and therefore knows a widespread application in the millitary, global possitioning systems, telemedicine, WiMax applications and so on. The authors of [18] also state that some of the disadvantages like lower gain and power handling can be solved with the usage of an array configuration.

The radiating patch is usually made of a thin layer of either gold or copper [17, 19] and can be any form. However, shapes besides a circle or rectangle would require large numerical computation [17]. A simple rectangular shape will thus be used. Further is also the dielectric constant of the substrate important which typically varies between 2.2 and 12. Finding a good dielectric depends on how the antenna will used. A lower dielectric constant with a thick substrate will result in better performance, better efficiency and larger bandwidths [19]. On the other hand, a larger dielectric constant reduce de dimensions of the antenna [17] which is also useful when attaching the antenna to a limited surface. Glass as a dielectric substrate with a constant of 4.4 will therefore be used.

3

Scenarios

The tool supports multiple configurations and the behavior will be different for most these configurations. Three main scenarios will be investigated, order based on the network complexity. Within each scenario, different configurations will be applied. For the first scenario, only one user with one drone will be present in the network. The network will thereafter be expanded for multiple users but with still only one drone available. Eventually, that last restriction will be dropped meaning that the third scenario covers multiple users with unlimited number of drones. Table 3.1 show the default configuration which values are always applicable unless mentioned otherwise.

3.1 A single user

This first scenario will investigate how SAR_{10g} and power consumption is influenced in an isolated environment meaning there is nor influence from other base stations nor other UE. The tool will provision one single drone and position it directly above the user. These results will however depend on the position of the user. If the randomly generated location of the user is indoor, the flying height of the drone might obstructed by the building where the user resides, causing the user to be uncovered. If this is not the case, the expected altitude of the user is half of the height of the building meaning that the user would be closer to the UABS as if he would

Broadband cellular network	
technology	LTE
frequency	2.6 GHz
Carrier	
carrier power	13.0 A
average carrier speed	12.0 m/s
average carrier power usage	17.33 Ah
carrier battery voltage	22.2 V
Femtocell antenna	
maximum P_{tx}	33 dBm
antenna direction	downwards (az: 0°; el: 90°)
gain	4 dBm
feeder loss	2 dBm
implementation loss	0 dBm
radiation pattern	EIRP or microstrip patch antenna
height	100m
UE Antenna	
height	1.5m from the floor
gain	0 dBm
feeder loss	0 dBm
radiation pattern	EIRP
number present in the network	224

Table 3.1: Overview of default configuration values.

have been outdoors. For a more consistent result, the user will therefore be positioned outside when systematically increasing the flying height.

Another considered variable will be the transmit power of the antenna. LTE makes usages of power control meaning that no more power will be used then strictly necessary. The actual transmit power therefore ranges between 0 and the maximum input power. This power is zero when either no user is present or the user is so far away that the actual transmit power would exceed the maximum transmission power. Increasing the maximum transmission power won't influence the power consumption or SAR_{10g} because the UABS won't use more then strictly required. It is therefore more useful to match the actual transmit power against a variable flying height.

This scenario investigates SAR_{10g}, power consumption and minimal transmission power. The used optimization strategy is not important. The optimization algorithm decides which user

will be connected to which drone in order to reach a certain goal. Since only one user and one UABS are available, both optimization strategies will behave identical. These values will be checked when using a fictional equivalent isotropic radiator and a realistic antenna.

The user gets a fixed position. The exact location doesn't matter as long as it is outside. For this experiment is choses for the 'Koningin Maria Hendrikaplein', a square just next to the train station of Ghent. Doing so will force the UE to always be at the same height of 1.5 meters. The conclusions will be based on SAR_{10g}, power consumption and transmission power. These output values depend on fly height and type of antenna. An overview can be found in table 3.2

Note that there is no explicit restriction on the number of drones in table 3.2. The deployment tool initialy places UABSs above each user and it is the optimzation strategy that decides which of these potentiol positions remain. Since there is only one user, there can also be only one drone.

Parameter	**Value**
x position user	3.711198
y position user	51.036747
shadow margin user	-3.0398193
number of users	1

Input variables	**Output variables**
type of antenna	SAR_{10g}
flying height	power consumption
	minimal P_{tx}

Table 3.2: Overview of the configuration.

3.2 Increasing traffic with only one drone available

This scenario investigate the same behavior as the previous. Still with one drone but for a higher number of users. The scenario can be divided into two groups. One for a variable flying height but with a fixed number of 224 users which is the number of active users on an average day at 5 p.m. meaning which means it is rush hour resulting in the highest number of simmulatanious users for the day[6]. The other scenario has a fixed flying height of 100 m as recommended by [6] but with a variable number of users. To enforce the tool to only use one drone, a facility capacity is set to one which implies that there is only one spot available in the facility where the UABSs are stored. The tool will still generate as much potential places as there are users in the network. But when the optimization algorithm is done, only one drone will remain.

Four possible configurations are possbile because there are two antennae available (equivalent isotropic radiator and a realistic antenna) which can both operate in an power consumption optimzed network or an exposure optimized network. These four configurations are investigated for the two groups mentioned above. Both groups can further be divided in four series where The SAR_{10g}, power consumption and user coverage will be investigated for both groups. The

Parameter	Value
facility capacity	1

Input variables	Output variables
type of antenna	SAR_{10g}
flying height	power consumption
number of users	user coverage
optimization strategy	

Table 3.3: Overview of the configuration.

only available drone will be positioned at the fly height of 100 m as recommended in [6]. For the second case, the same output variables are investigated for a varying fly height but with a fixed number of 224 users. Both cases will be investigated for the two types of antennae: the fictional equivalent isotropic radiator and the microstrip patch antenna.

3.3 Increasing traffic with an undifend amount of drones

Input variables	Output variables
type of antenna	SAR_{10g}
flying height	power consumption
number of users	user coverage
optimization strategy	

Table 3.4: Overview of the configuration.

When more drones are available, an optimization strategy can be applied. The tool checks the capacity of the basestations and decides thereafter wich basestation the user should be connected to. The original algorithm checks all pahts between the user that need to be connected with all drones. Thereafter, the drones which path experience the least pathloss and still has the capacity to cover an addition user will be selected. The authors from [11] proposed however annother optimization strategy which tries to minimize electromagnetic exposure and power consumption.

The input variables flying height, transmit power and number of users will be used to see how electromagnetic exposure, power consumption en number of drones are influenced for different optimization strategies and type of antennas.

Since there is no fixed budget limitation, the number of drones are unlimited. The tool will therefore try to connect each user and coverage will be expressed in number of drones required to cover as much users as possible instead of having a limited number of drones as in scenario and therefore has only a limited coverage expressed in percentage.

4

Methodology

4.1 Tool

The goals

4.2 Electromagnetic exposure

4.2.1 Calculation of the total specific absorption rate

The total whole body SAR (SAR_{10g}^{wb}) of a user can be calculated by a simple sum of individual SAR values from the different sources. Forumula 4.1 was originally described in [14] for SAR values induced into the head. Using SAR_{10g}^{head} would however result into incorrect conclusions since the position of the phone relative to the user is unknown. This is because the tool assigns a bitrate to a user depending on the service he is using meaning that users in the network are not only calling but are able of using other services as well like browsing the web. The induced electromagnetic radiation will therefore be expressed in function of the entire body.

$$SAR_{10g}^{wb,total} = SAR_{10g}^{wb,ul} + SAR_{10g}^{wb,dl} + SAR_{10g}^{wb,neighbours} \tag{4.1}$$

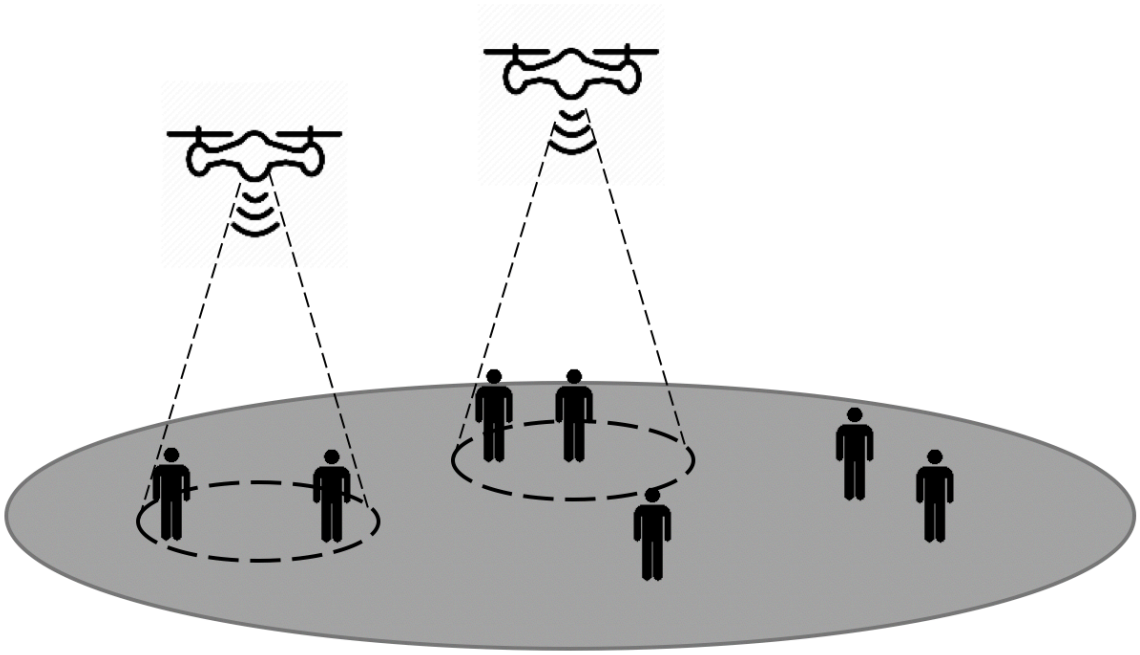

Figure 4.1: Design of the microstrip patch antenna.

The first parameter, $SAR_{10g}^{wb,ul}$, will indicate the absorbed electromagnetic radiation by the entire body originating from the user's own device whereas the second parameter $SAR_{10g}^{wb,dl}$ will represent the absorbed electromagnetic radiation caused by all the base stations in the considered area. The last factor, $SAR_{10g}^{wb,neighborhood}$, specifies the exposure of our user from the UL radiation from other mobile devices.

4.2.2 Electromagnetic exposure caused by far-field radiation

Electromagnetic exposure to which people are exposed can be categorized in two groups. One of them is near-field radiation which is caused by the users own device and which will be discussed in 4.2.3. The other type is far-field radiation and will be explained in this section. This kind of radiation is caused by radiators 'far away'. Examples of these types of radiators are UE which belong to other people and UABSs.

Electromagnetic radiation from a single source

To determine the total exposure of a single human being or even of the entire network, the electric-field $\vec{E}$ from a single radiator i should be calculated. The formula to determine this

electromagnetic value E (expressed in V/m) for a specific location u is given in equation 4.2.

$$E_i(u) = 10^{\frac{RRP(u)-43.15+20*\log(f)-PL(u)}{20}} \tag{4.2}$$

frequency The used frequency in the formula above is denoted as f and is expressed in Mhz. Since LTE is used, this value will be 2600.

Real Radiation Power and EIRP In the original formula of 4.2 as it was described in [11, 10] was RRP defined as Equivalent Isotropical Radiation Power (EIRP). An EIRP is a theoretical source of electromagnetic waves which radiates the same intensity for all directions. The formula to find this EIRP value is described in 4.3 where P_t stands for the input power of the antenna, G_t for the gain of the transmitter and L_t being it's feeder loss.

$$EIRP = P_t + G_t - L_t \tag{4.3}$$

This formula, constructed out of different gains and losses, misses a factor when accounting for real life radiation patterns. Therefore makes formula 4.2 usage of RRP instead of EIRP and can be defined as follows:

$$RRP(u) = EIRP - attenuation(u) \tag{4.4}$$

The attenuation for the user u is given based on the angle between the main beam and the user. More details on how this can be implemented is described in 4.4.2 Thereafter, the attenuation can simply be subtracted from the EIRP-value, when assuming that $attenuation(u)$ returns positive values. When assuming that

path loss At last, formula 4.3 requires the path loss (dB). In order calculate the path loss, an appropriate propagation model is required. Several propagation models exists and the tool already uses the Walfish-Ikegami model [6]. This is because the Walfish-Ikegami model performs well for femtocell networks in urban areas. The chosen propagation model consists of two formulas depending on whether a free line of sight between the user and the base station exist or not. Both formulas expect a distance in kilometer.

input power hangt af van bs tot bs.

Combining exposure

The electromagnetic exposure for a given location originating from different sources can be calculated with formula 4.5 (in V/m). E_i stands for the electromagnetic exposure from source i

and n stands for all far-field radiators of a certain category which will either be UABSs or UE. E_{tot} was originally calculated for each x meters [11]. In the tool, the exact location of the users in known and E_{tot} will thus only be calculated for locations where a user is positioned.

$$E_{tot} = \sqrt{\sum_{i=1}^{n} E_i^2} \tag{4.5}$$

Weighted avg

write about weighter average of hoort dit bij decistion algo?

Converting far-field electromagnetic exposure to SAR_{10g}^{wb}

Formula 4.1 expects that the electromagnetic radiation expressed into $SAR_{10g}^{wb,dl}$ and $SAR_{10g}^{wb,neighbours}$. The calculation for both values are in fact identical. The difference is the sources where the first one is for UABSs and the second one for UE. Physically seen, they are both whole body SAR values induced by far-field radiation $SAR_{10g}^{ff,wb}$

The electromagnetic radiation needs to be converted. This conversion constant is based on Duke from the Virtual Family. Duke is a 34-year old male with a weight of 72 kg, an height of 1.74 m and body mass index of 23.1 kg/m [15]. Research shows that the conversion factor for WiFi $0.0028\frac{W/kg}{W/m^2}$ is. Since WiFi at a frequency of 2400 Mhz is very close to LTE at 2600 Mhz, it is assumed in [15] that these values are also applicable for LTE. This constant converts converts power flux density S (with units $\frac{W/kg}{W/m^2}$) to the required $SAR_{10g}^{ff,wb}$ but the electromagnetic exposure from formula 4.5 is expressed in V/m instead of the power flux density in W/m^2 and should therefore be converted first using formula 4.6 after which formula 4.7 can be applied.

$$S = \frac{E^2}{337} \tag{4.6}$$

$$SAR_{10g}^{wb,dl} = S * 0.0028 \tag{4.7}$$

4.2.3 Electromagnetic exposure caused by near-field radiation

When an user is active, electromagnetic exposure won't be limited by DL traffic from UABS or UL traffic from other UE but also from UL traffic from his own device. This radiation should also be accounted for. However the radiation from UL traffic is destined for the serving UABS, a part of that radiation enters the user's body.

Localized Specific Absorption Rate

When assuming that all users hold their device next to their ear, a localized SAR-value for the head SAR_{10g}^{head} can be calculated. International Electrotechnical Commission (IEC) defines in IEC:62209-2 a maximum for a 10g tissue SAR_{10g}^{head} as 2 W/kg and a maximum for a 1g tissue SAR_{1g}^{head} as 1.6 W/kg. Most countries, including Belgium, enforce the 10g model and will, therefore, be the point of reference for this master dissertation. The SAR_{10g}^{head} values are phone dependent. The reported values by companies of mobile devices are worst-case scenarios meaning that the values are measured when the phone is transmitting at maximum power. This is an understandable decision but won't result in a realistic scenario since modern cellular networks use power control mechanisms to prevent over radiation of a nearby device. UE will therefore never use more energy than necessary to maintain a connection. To compensate for this overestimation, the actual SAR_{10g}^{head} of each user will be predicted. These will, however, remain an estimation since the position of the phone related too the head differs from user to user. For example, by holding the phone differently, a hand can absorb more or less electromagnetic radiation. TODO: bron.

$$SAR_{10g} = \frac{P_{tx}}{P_{tx}^{max}} * SAR_{10g}^{max} \tag{4.8}$$

Equation 4.8 is used to predict the actual SAR_{10g}^{head} of a certain user. T

The maximum transmission power P_{Tx}^{max} for a phone in LTE and UMTS is 23 Dbm [20, 12]. The actual transmitted power by the UE, is predicted with equation 4.9.

$$P_{Tx} = P_{sens} + PL \tag{4.9}$$

The SAR_{10g}^{max} value is different for each mobile device. An average is calculated based on 3516 different phones from various brands using an German database [21] for which an overview can be found in fig. 4.2. When the phone is positioned at the ear, an average of 0.7 W/kg is found with a standard deviation of 0.25 W/kg which are very similar results as in Ref. [22]. The median of 0.67 is used.

Whole body specific absorption rate

The position of the phone compared relative to the user is unknown. The tool assigns different bitrates to different phones implying that some users re calling and therefore probably holding their phone next to their ear wile another part is using other services like browsing the web. The SAR_{10g} caused by the user's UL traffic will for this reason be expressed in function of the entire body. For this reason expects formula 4.1 that the specific absorption rate is expressed for the entire body instead of localized SAR_{10g}^{head}. Therefore, the conversion factor from [15] for

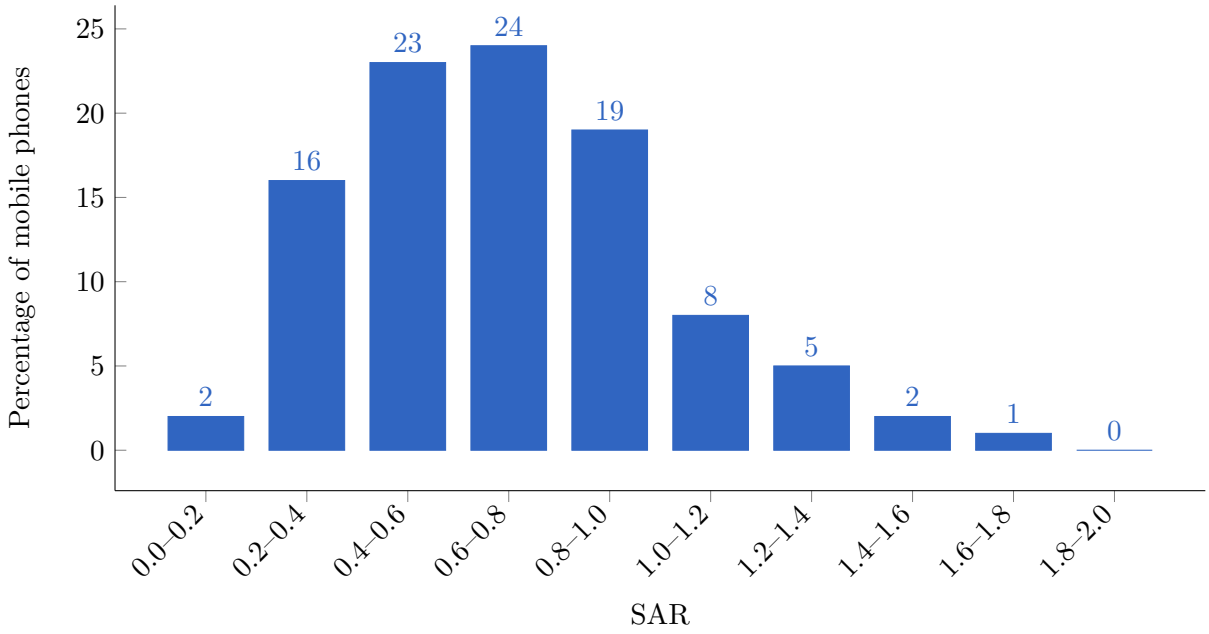

Figure 4.2: Distribution of how many phones belong to a certain SAR interval. Upper boundary not included

WiFi is reused as which was already the case in 4.2.2.

$$SAR_{10g}^{wb,ul}\left(\frac{W}{kg}\right) = 0.0070\left(\frac{W/kg}{W}\right) * P_{tx}(W) \tag{4.10}$$

4.2.4 Defining an antenna

A microstrip patch antenna is chosen because it allows easy production but more important it has a low weight and has a thin profile causing it to be very aerodynamic which is useful when attaching it to an UABS [18].

The dimensions of the antenna depend on the frequency it is operating and the characteristics of the used substrate. The antennas will be radiating at a center frequency f_0 of 2.6Ghz. A substrate with a higher dielectric constant and low height reduces the dimensions of the antenna and a lower dielectric constant with a high height improves antenna performance. The used substrate will therefore be glass with a dielectric constant of 4.4. The height of the antenna is also limited to 2.87 mm in order to keep the antenna light and compact [17]. The formulas from [17] are [19] applied.

description	symbol	value
center frequency	f_0	2600 Hz
dielectric constant	ϵ_r	4.4
heigt of the substrate	h	0.00287m

Table 4.1: Overview of configuration parameters

$$W = \frac{c}{2 * f * \sqrt{\frac{\epsilon_r + 1}{2}}} \tag{4.11}$$

Which C the speed of light, f being the center frequency of 2600 Hz and a dielectric constant of $\epsilon_r = 4.4$ a width of 3.51 mm is achieved.

$$\epsilon_{reff} = \frac{\epsilon_r + 1}{2} + \frac{\epsilon_r - 1}{2} * \left(1 + 12 * \frac{h}{W}\right)^{-\frac{1}{2}}$$

The height of the dielectric is choses to be 2.87mm in order to keep the antenna small and light**??**. ϵ_r is the permittivity constant of the substrate and depends of the used material. In this paper, a substrate like glass is chosen because of the high dielectric constant of $\epsilon_r = 4.4$ compared to other materials like teflon with only a dielectric constant of $\epsilon_r = 2.2$. This is because larger dielectric decreases the dimensions of the antenna patch **??** and therefore indirectly also decreases the dimensions of the entire antenna surface which comes in handy for the limited space on drones. When substituting these values, a ϵ_{reff} of 3.91 is determined.

$$L_{eff} = \frac{c}{2 * f * \sqrt{\epsilon_{reff}}} \tag{4.12}$$

Applying this formula with the known values of above the L_{eff} results in 29.16 mm.

$$\Delta L = 0.412 * h * \frac{(\epsilon_{reff} + 0.3)\left(\frac{W}{h} + 0.264\right)}{(\epsilon_{reff} - 0.258)\left(\frac{W}{h} + 0.8\right)} \tag{4.13}$$

By substituting the values from above, the length extension determines that ΔL equals 1.3071 mm.

Finally can the length of the patch be calculated using the expression: $L = L_{eff} - 2 * \Delta L$ which result in 26.55 mm which result in an antenna like 4.3.

The transmission line model is in fact only applicable for an infinite ground plane but it has been proven that similar results can be achieved if the ground plane's dimensions are bigger

then the patch of approximately 6 times the height of the dielectric substrate [17, 19].

$$L_g = 6 * h + L \tag{4.14}$$

$$W_g = 6 * h + W \tag{4.15}$$

Therefore should the length of the ground plane L_g be at least 0.0438m and a width of W_g 0.0524m.

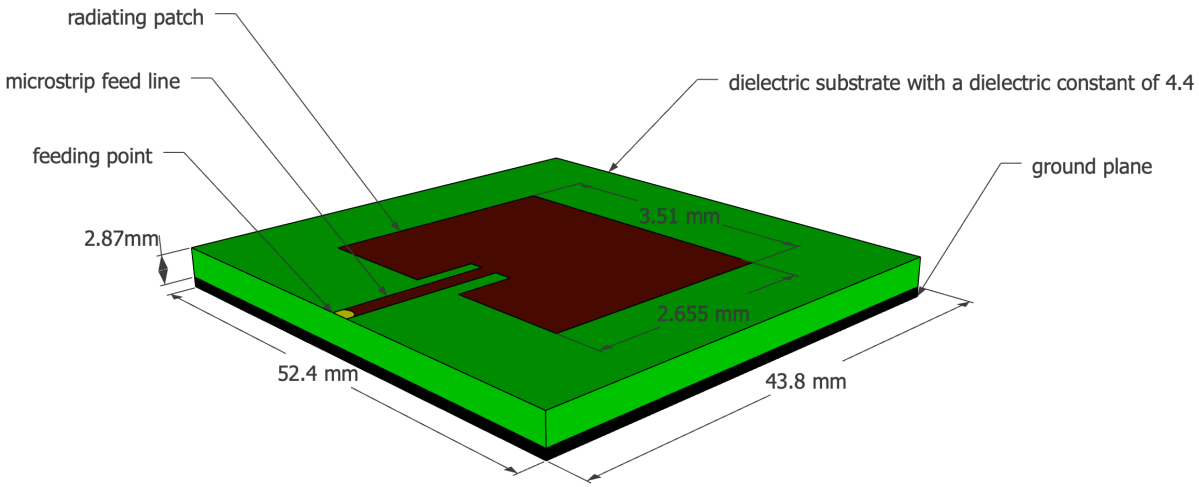

Figure 4.3: Design of the microstrip patch antenna.

4.2.5 Radiation pattern

Mathlab is able to generate the radiation pattern for the this microstrip patch antenna. The code in 1 starts with defining the dielectric substrate which will be glass with a dielectric constant of 4.4 and a height of 0.00287m. Thereafter is the microstrip patch antenna generated with the width and length being the dimensions of the radiation patch and the `GroundPlaneLength` and `GroundPlaneWidth` the dimensions of the ground plane and dielectric substrate. The `FeedOffset` is the relative offset from the center where the radio frequency power is fed to the radiating patch which here wil be at the edge which is in figure 4.3 is indicated with the yellow dot. At last is the dielectric object given to the `patchMicrostripInsetfed`-object.

Generating the pattern is done with the `pattern`-command. The first value is the `patchMicrostripInsetfed` object followed by the frequency in which the antenna will be operating. Optionally can a azimuth value be parsed like in line 7 and 8 where 90 and 0 stand for relatively the H-plane and E-plane.

```
d = dielectric("Name",'glass',"Thickness",0.00287,"EpsilonR",4.4)
p = patchMicrostripInsetfed("Width",0.0351,"Length",0.02655,
    "GroundPlaneLength",0.0438,"GroundPlaneWidth",0.0524,
    "FeedOffset",[-0.021885 0],"Substrate", d)

pattern(p,2.6e9, "CoordinateSystem", 'polar', "Normalize",true)
pattern(p,2.6e9, 90, "CoordinateSystem", 'polar', "Normalize",true)
pattern(p,2.6e9, 0, "CoordinateSystem", 'polar', "Normalize",true)
```

Listing 1: Mathlab code to generate radiation pattern for a microstrip patch antenna

Running the configuration from 1 will generate the radiation pattern from figure 4.4. When running the same configuration for a slightly bigger square antenna with an edge of 0.060m, the radiation pattern from 4.5 is achieved. It becomes clear that the radiation pattern from figure 4.4 has a higher attenuation in de direction it is not facing compared to the radiation pattern of figure figure 4.5. If it is assumed that drones fly lower then users are positioned in some buildings, the pattern of 4.4 would be a better approach. However, for the continuation in this master dissertation, the radiation pattern from figure 4.4 is assumed since the antenna is the smallest and therefore more suitable to attach to the limited space available under the drone. A data sheet of the exact values from both radiation patterns can be found in appendix A.

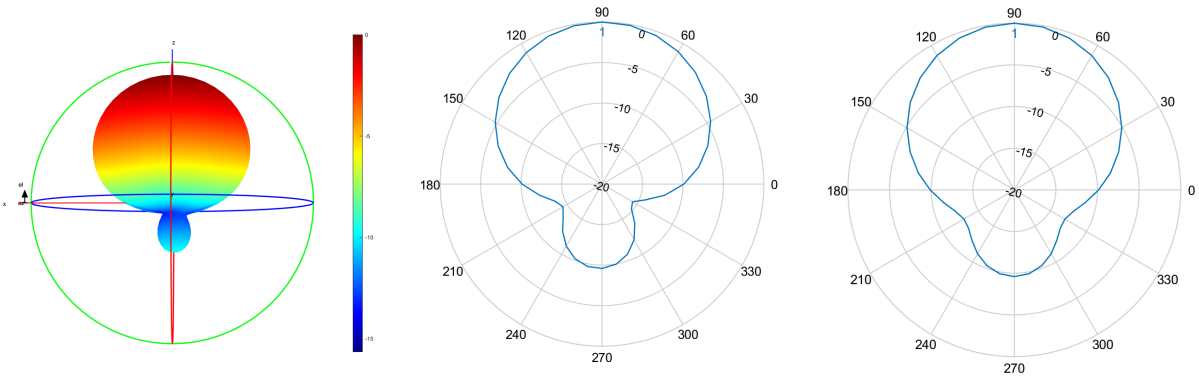

Figure 4.4: Radiation pattern 1: 3D model of the entire pattern on the left with the configuration as described above. In the middle a 2D radiation pattern of the E-plane and at the right a 2D model of the H-plane.

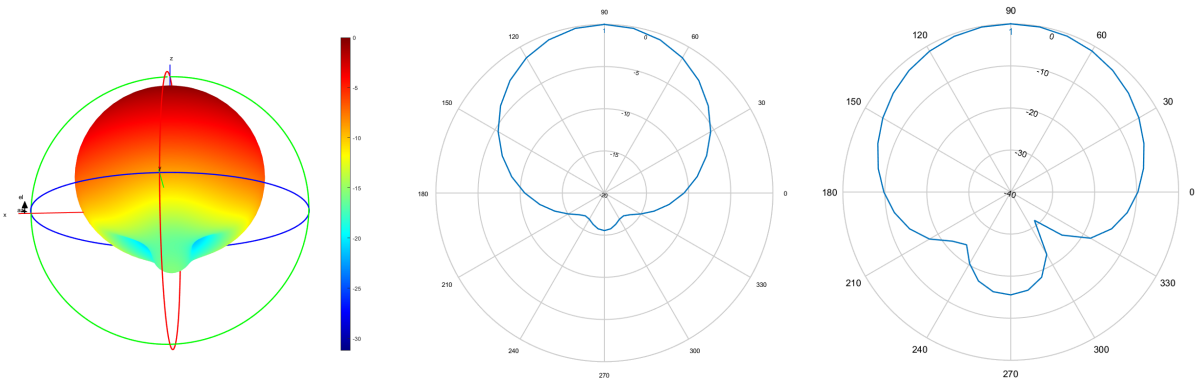

Figure 4.5: Radiation pattern 2: Generated with a groundplane of 0.06m by 0.06m. On the left is the 3D model of the entire pattern plotted. In the middel a 2D radiation pattern of the E-plane and at the right a 2D model of the H-plane.

4.3 Optimizing the network

The network as originally defined in the deployment tool tried to minimize power consumption by connecting the user to a base stations which experienced the lowest path loss. A second optimization strategy is introduced, based on the fitness function described in [11].

$$f = w * \left(1 - \frac{E_m}{E_{max}}\right) + (1 - w) * \left(1 - \frac{P}{P_{max}}\right) * 100 \tag{4.16}$$

Formula 4.16 returns a fitness value. Users are connected to different UABSs and each time the fitness value is calculated. The user will eventually be connected to the drone which resulted in the highest fitness value. This process is repeated for each user. w is the importance factor of electromagnetic exposure ranging from 0 to 1 with boundaries included. A w set to zero means that electromagnetic exposure is not important and therefore be called an power consumption optimized network. Likewise, a w set to one will be called an exposure optimized network. P_max is the power consumption if all UABSs are active and would be radiating at the highest possible level and P the used power by the current network. This will be the power required for the flying drones themselves and there antennae. E_m will be the exposure for the current designed network and E_{max} the electromagnetic exposure when all antennae are at their highest power level.

The weighted average E_m can be found by inserting the median and 95 percentile from all exposures into formula 4.17. Since the location of all users in the deployment tool are known,

it is sufficient to calculate exposure only in those positions.

$$E_m = \frac{w_1 * E_{50} + w_2 * E_{95}}{w_1 + w_2} \tag{4.17}$$

w_1 and w_2 in 4.17 being the weighting factors. Not only the median exposure is important but also limiting higher exposure is important. Just like [11] is with that reason w_1 and w_2 chosen to both have an equal importance of 50 %. todo: in J1 is dit gedetailleerder uitgeschreven. Mogelijk om hier wat extra over te schrijven.

4.4 Implementation

4.4.1 Network planning

TODO Thereafter, all inactive users are deleted and only the x best bs are kept with x equal to facilityCapacity. Eventually, exposure is one last time calculated and objects are initialized with the correct exposure values.

4.4.2 Implementation of the radiation pattern

The deployment tool originally only supported EIRP antennas. The tool thus has been extended and is fully configurable allowing any possible antenna in any possible orientation using the XML-file describing the femtocell. The configuration described in this file applies to all UABSs.

The orientation is done using two values called 'downtilt' and 'north offset'. The first value defines the downtilt angle under wich the antenna is pointing. An angle of 0 degrees is perfectly horizontal and pointing straight to the ground is done with an angle of 90°. This parameter only supports positive values ranging from 0° to 360° (upper boundary not included). An antenna pointing to the sky would therefore require a value of 270°. The second value, the north offset, defines the azimuth orientation of the drone. The value given to this parameter indicates the offset between the north and the horizontal direction the antenna should be pointing to. The value should once again range from 0° to 360° with the upper boundary not included. The angle is calculated in counter clock wise orientation. For instance, a north offset of 270° will let the UABS point to the east.

Thereafter, the normalized radiation pattern is supplied to the tool. The actual pattern is three dimensional. To simplify this, slices perpendicular to the az-axis are extracted. These are indicated at figure 4.6 with azimuth cut. With an angle of 90°, four slices are achieved, each

consisting out of elevation cuts. The intersection of an elevation and azimuth plane corresponds with a certain attenuation which is fed to the tool. Figure 4.6 show only 3 elevation planes. The radiation pattern used in the tool has an attenuation every 10°. In other words, a slice consist of 19 values ranging from 0° to 180° (boundaries included).

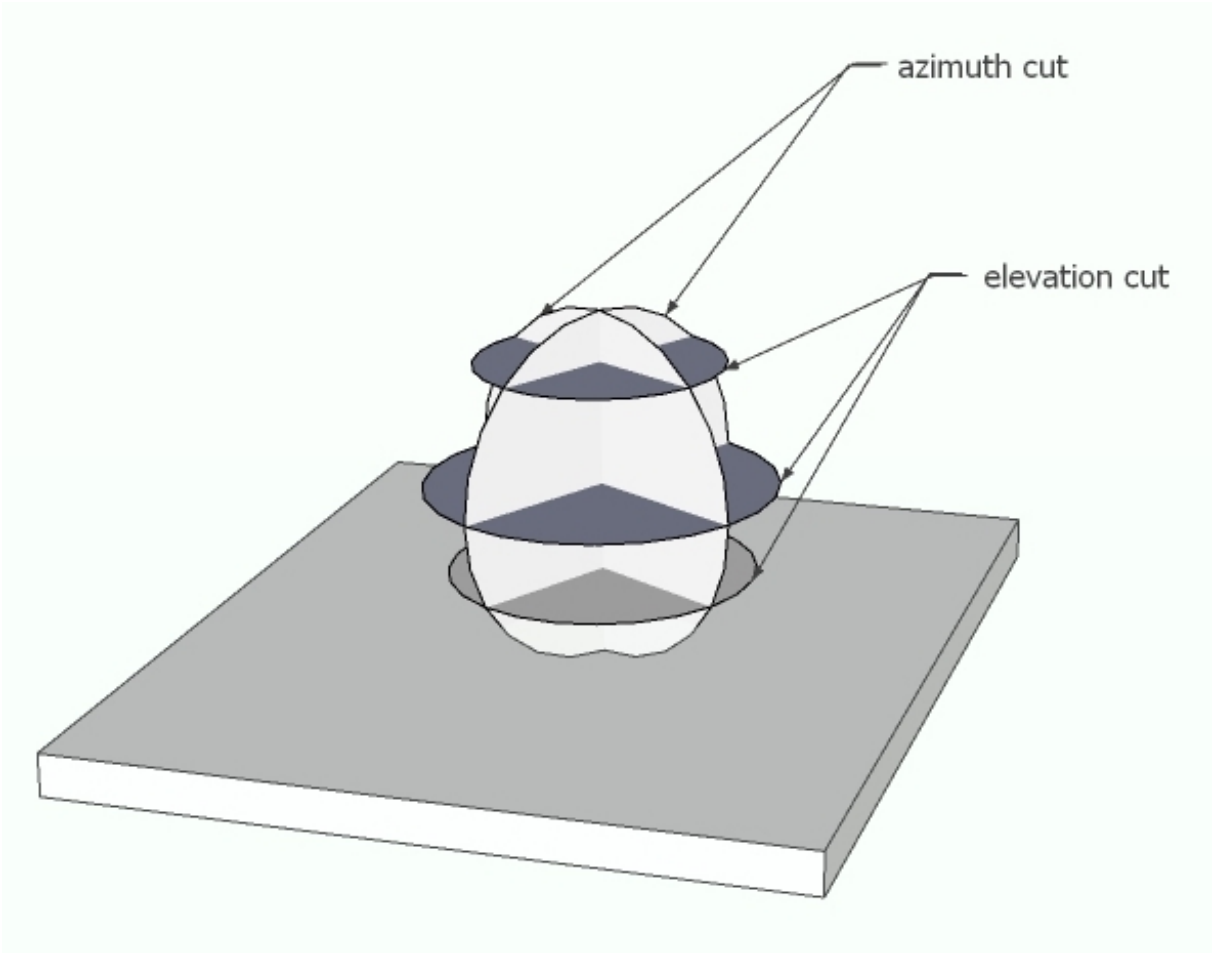

Figure 4.6: Schematic example of slices in a radiation pattern.

The number of required sliced depend on the complexity of the radiation pattern. For symmetrical radiation patterns like in figure 4.4 and 4.5, two cuts perpendicular to each other dividing the radiation pattern in 4 azimuth-slices is definitely sufficient. However, this might not be the case for radiation patterns with a more complex structure contains several side lobs. To tackle this issue, more azimuth-slices can be defined for increased precision. Each slice should however contain an equal amount of elevation slices. A concrete example of a configuration file can be found in appendix B.

TODO: maak onderstaande tekst samenhandend. Hij begint altijd met ”the”

When the attenuation of a user to a certain UABS needs to be known, the elevation and azimuth angles between the user and the antenna's direction will be calculated. This user is indicated in figure 4.7 with a black dot. The small black lines represent azimuth and elevation planes. The tool knows the exact attenuation only at the intersection of those lines. The change that the user is positioned at such an intersection is very small. The attenuation for the requested point can be estimated using bilinear interpolation. First, the attenuation is estimated for the intersection of the red-orange line using linear interpolation on the horizontal axis using the known values at the end of the red line. The same is done for the orange-green intersection using the known values at the end of the green line. Finally, linear interpolation is used in the y-git status direction using the estimated values at the end of the orange line.

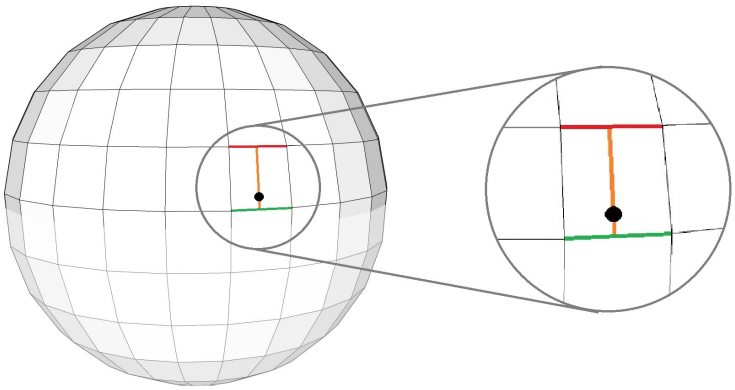

Figure 4.7: Schematic example of how bilinear interpollation works.

4.4.3 Performance improvement

Calculating path loss

The path loss is required for several formulas. For instance, each user decides whether a UABS is feasible based the path loss but also the calculations for the downlink electromagnetic exposure require this value to be known. The formulas for the whole body SAR_{10g} require not only the path loss between the user and all UABSs but even the path loss between users themselves. These path loss calculations are based and the Walfisch-Ikegami Model and makes a distinction between line-of-sight and non-line-of-sight situations causing a high computational load. The calculation between two points stands completely free from any other calculation between any other point and is therefore a suitable candidate to be multithreaded. The deployment tool creates two thread pools. The first pool creates a thread for each user where each thread calculates the path loss between the user assigned to him and all possible UABSs causing a time complexity of n^2. Each user stores all path losses between himself and any other UABS and result therefore in a total space complexity of n^2. When all users are finished, the pool is shut

down and a second one is created for the same calculations but between users. The pool will, just like the previous, create threads for each user but has an important difference. When a certain user calculates the path loss to another user, this path loss also applies for the other direction. The tool saves time by calculating the path loss only once and stores the path loss with both users. It is therefore sufficient that a given user only calculates path losses to users left of him, since the other will be calculated by the users right to him. This results in a time complexity of only $n(\frac{n}{2})$. When the last user finishes his thread, all users know the path loss to all other users causing a space complexity of $n(n-1)$.

Limiting antenna searching

The user needs to be connected to the 'best' base station. To identify this best UABS, the user should be connected to each base station and the fitness value 4.16 of the network should be evaluated. The connection which resulted in the best fitness function will be added in the solution. This process is repeated for each user but can further be improved. A user will likely be connected to either UABS directly above him or to a UABS in the direct neighborhood. Time complexity can thus be improved by not considering drones outside a certain radius. An ideal data structure for neighborhood-search is a KD-tree. This data structure is based on a binary tree and optimal for objects with multiple keys. Objects are thus positioned in K dimensions, each node split the hyperplane over exact one dimension. The dimension that need to be split depends on the level of the KD-tree where that node is situated. In this case, the x and y coordinate will be used in a 2D-tree (k=2) like in figure 4.8.

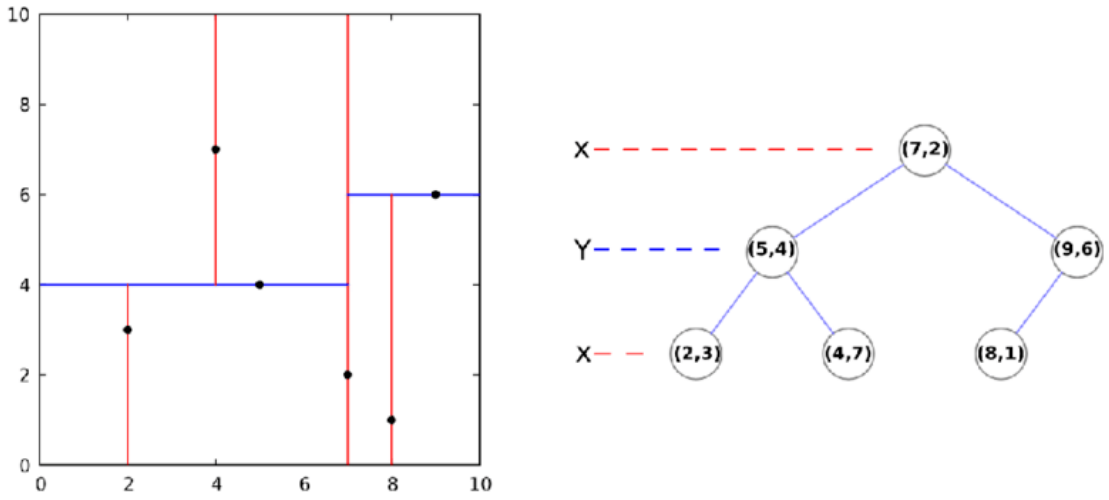

Figure 4.8: Example of a KD-three in two dimensions

Here, is chosen to consider only UABSs within a radius of half a kilometer. In a scenario of 500 UABSs, 60 possible UABSs are verified. TODO: schrijf ook voor 200 users.

5

Results and discussion

5.1 Number of simulations

The algorithm makes usage of randomly distributed users causing each simulation to be difference. The results are based on average values over multiple simulations. It is therefore important knowing how mush simulations is required in order to become a converged average. This is done by using an example scenario which details can be found in table **??**. The most important parameters investigated in the different scenarios are SAR_{10g}, power consumption and user coverage. Therefore, the cummulative avarage of each investigated value is plotted in function of number of simulations.

Parameter	value
number of users	40
facilityCapacity	20
fixedFlyHeight	100
optimization strategy	power consumption optimized

Table 5.1: Overview of the configuration.

The number of simulations has a direct influence on the runtime. Certain configurations take a considerable amount of runtime (expessed in hours). This is because of the exponential time

complexity. The deployment tool with n users, will need to calculate n times the pathloss between n drones and n users and thereafter $n/2$ times between each user. Thereafter, each user will have to be connected to the best possible UABS and each user is therefore required to consider multiple UABSs.

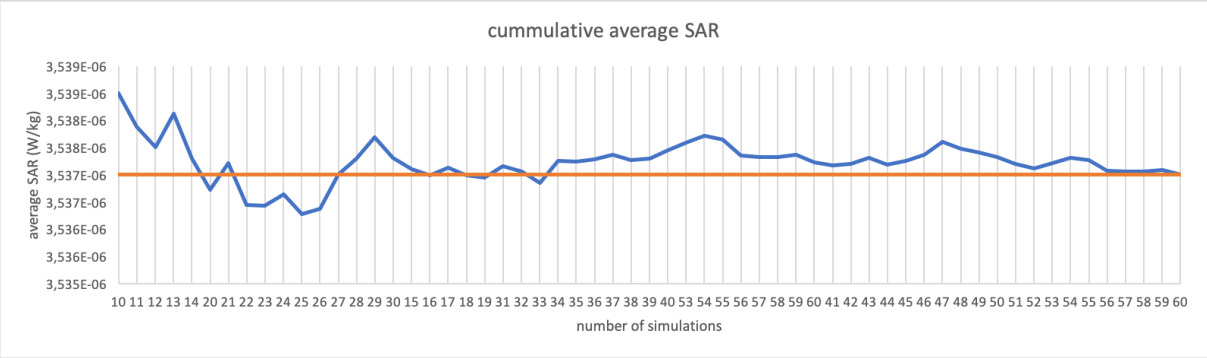

Figure 5.1: General design of a microstrip antenna

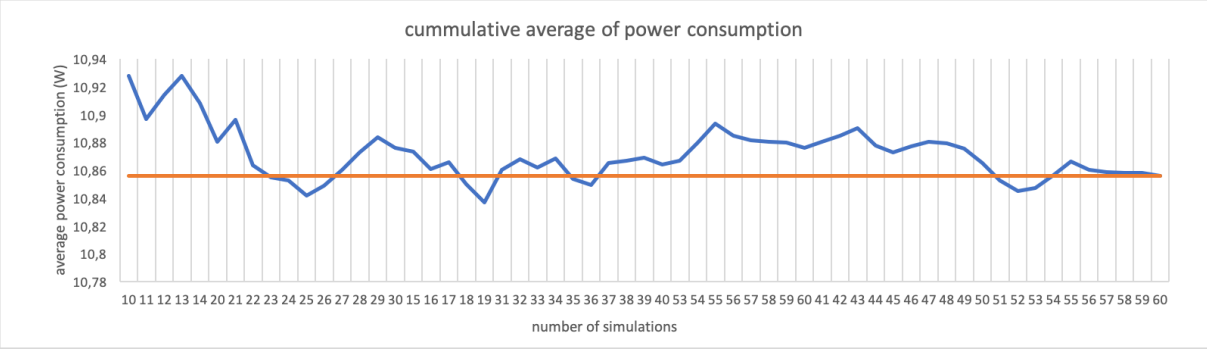

Figure 5.2: General design of a microstrip antenna

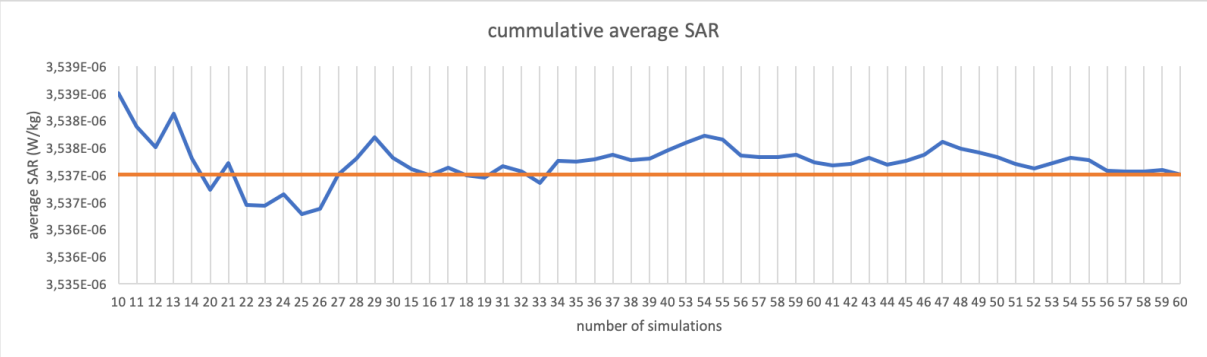

Figure 5.3: General design of a microstrip antenna

5.2 Scenario 1: one user and one base station

5.2.1 The influence from the maximum transmission power

LTE makes usages of power control meaning that no more power will be used then strictly necessary. The actual transmit power P_{tx} therefore ranges between 0 and the maximum input power. P_{tx} is zero when either no user is present or the user is so far away that the actual transmit power would exceed the maximum transmission power. Increasing the maximum transmission power won't influence the power consumption or SAR_{10g} because the UABS won't use more then strictly required. It is therefore more useful to match the transmission power against a variable fly height. Figure 5.4 shows a logarithmic relationship showing that P_{tx} increases fast at low altitude but slows down at lower altitudes.

Figure 5.4 shows the minimal required energy by an equivalent isotropic radiator in other to reach the user just below him. As already discussed in 3.1, the user is outdoor and just below the UABS. There is thus a free line-of-sight between both radiators. It is clear that a step function is achieved from this. This is because multiple flying heights correspond to the same flying height. When the flying height increases, so does the pathloss. LTE tries to counteract this by increasing the power level. Each time the pathloss becomes to high, the power level of the antenna increases with one dBm. Doing so, decreases pathloss allowing the antenna to reach the user again. When the flying height immediately after increases again, the pathloss also increases but not enough to force the drone to increase his power level again. This explains the discontinue step function. If the tool would make usage of smaller step size, a more continuous logarithmic function would be achieve. This would however worsen the time complexity because increasing the power level to exceed the pathloss happens in smaller steps. The red line indicates the default maximum transmission power used during simulations. In a free line-of-sight scenario with only one user, a UABS can fly up to 387 meters before losing connection.

This scenario is investigated with a microstrip patch antenna using power consumption optimization. However, these parameters does not matter. While an equivalent isotropic radiator no attenuation, a microstrip patch antenna does but since the user positioend in the perfect center of the main beam there won't be any attenuation in eighter cases. Also the optimization wont' make a difference. The goal of the strategy is to decide wich drone is most suitable for which users. Since there is only one user and one possible position for the drone, both optimization strategies behave identical.

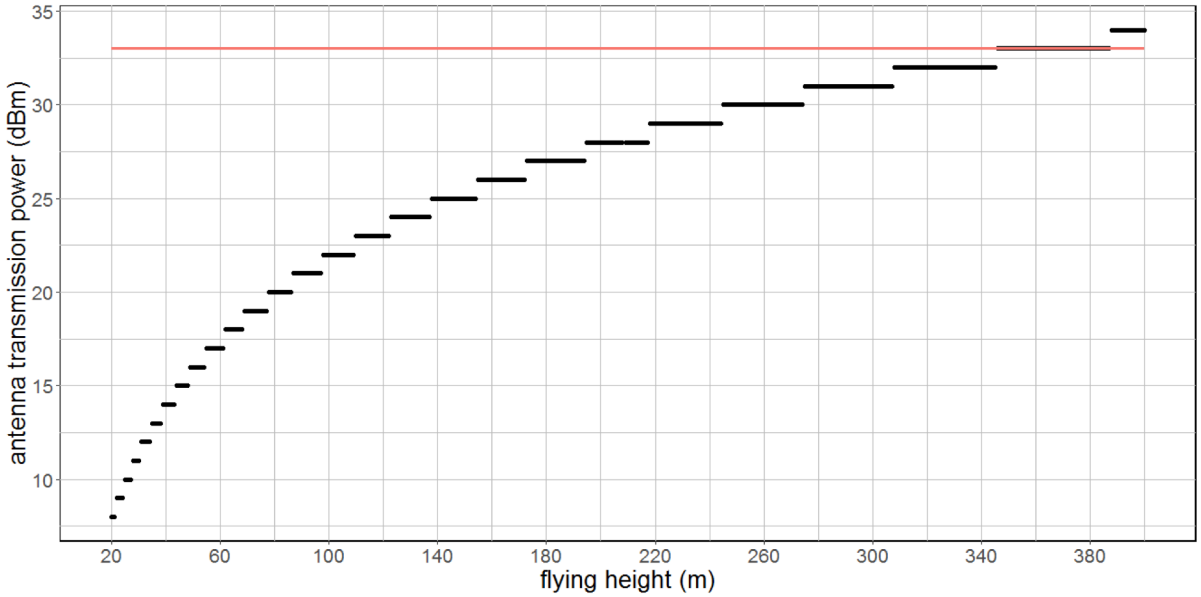

Figure 5.4: Minimal required transmission power by the antenna to reach the ground just below him.

5.2.2 Influence of the flying height

This section investigates how the fly height of the UABS influence SAR_{10g} and power consumption. In figure 5.3 becomes clear that with an increasing flying height, the specific absorption rate grows exponentially which is also the case for the power consumption (fig. 5.6)

Figure 5.5 shows the induced electromagnetic radiation for our user. The red line shows the $SAR_{10g}^{owndevice}$. This radiation very low when the UABS is close to the ground but increases exponentially at higher flying altitudes. The green line represent the $SAR_{10g}^{basestation}$ which shows the same discontinue behavior from in figure 5.4. As explained before, LTE makes usage of power control. Meaning that the power transmission only increases when pahtloss increases up to the point where the power level exceeds its maximum after which connection is lost completely and exposure drops to zero. This behavour causes the electromagnetic radiation experienced by the user to be almost constant. The slightly visible variation is just an extention of the reason why figure 5.4 forms a step function. When the power level increases with $1dBm$, it is more then strictly required causing the electromagnetic radiation to slightly increase. Just before an energy jump, pathloss and power level are perfectly balanced generating the lowest possible electromagnetic radiation possible.

Figure 5.5 doesn't show radiation from neighbours, because there are non present in this scenario. Finally, all these values are added as explained in formula 4.1.

The figure shows that for low flying drones, UABSs are the main source of electromagnetic radiation. This changes around 80 meters where UL electromagnetic radiation of the UE exceeds DL radiation in order to still be able to reach the high flying UABSs.

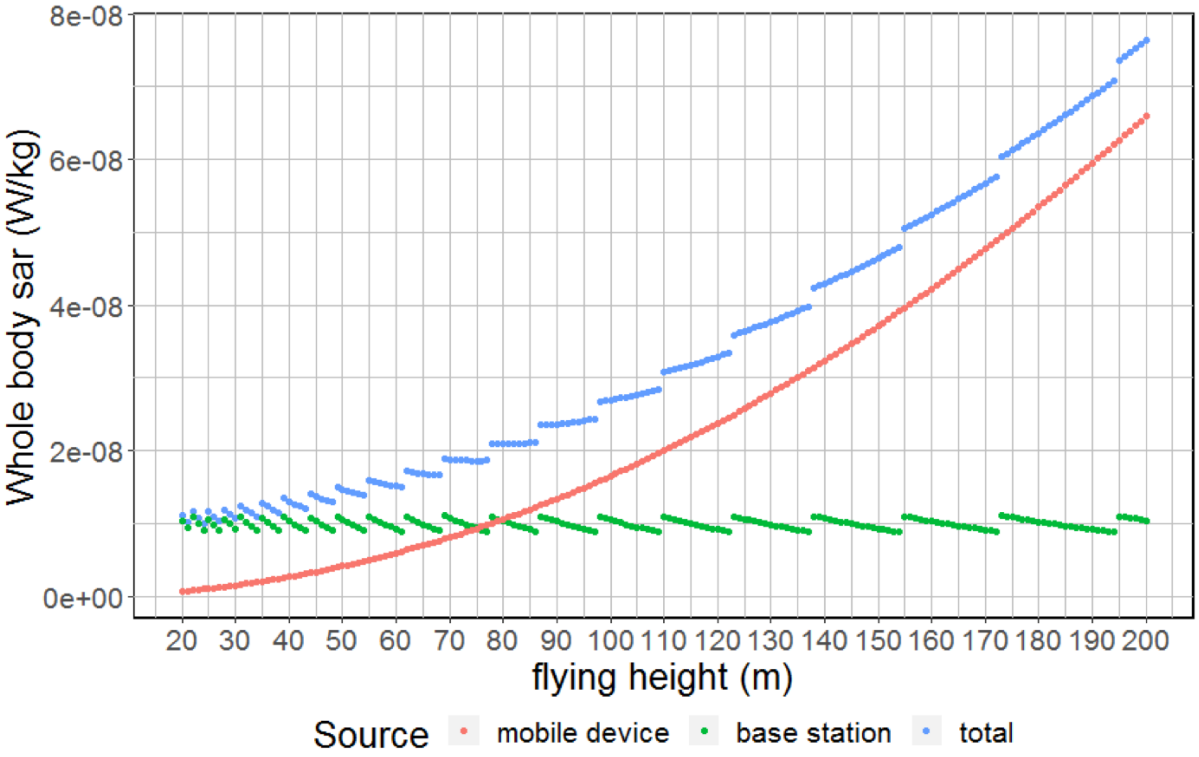

Figure 5.5: General design of a microstrip antenna

5.3 Scenario 2: increased traffic

5.3.1 Influence of the flight altitude

This scenario investigates how the network consisting of one UABS behaves when applied on an ordinary day during rush hour. On average, 224 active users are distributed uniformly over the city center of Ghent. Chart 5.7 shows how the downlink exposure is influenced by flying height of the UABS. Increasing the flying height has a direct influence on the total downlink exposure of an individual user. This is because if a drone flies higher, there is less penetration loss from obstructing buildings.

A power consumption optimized network with an EIRP antenna (yellow) has the highest exposure. This is logical when comparing with an EIRP antenna in an exposure optimized network (red). However, when looking at chart 5.8, the power consumption in a power consumption optimized network is worse than in an exposure optimized network. To understand this, the be-

havior of the deployment tool needs to be understood first. We know that a power consumption optimized network will result in few high powered UABSs while an exposure optimized network generates a lot of low powered UABSs. When only limited amount of UABSs are available, like only one in this scenario, the tool will only keep UABSs which cover most of the users. Therefore, is the power consumption in a power consumption optimized network way higher.

Chart 5.9 shows that the flying height has a positive influence on the user coverage. When a UABS flies higher, there is less pathloss between the user and the drone caused by buildings. As mentioned before, a power consumption optimized network will result in few high powered UABSs. The tool removes all UABSs except the one with most users. The network therefore exist out of one high powered UABS compared to the exposure optimized network with one drone which will be less powered. Since yellow has a higher power level, also more users will be covered.

When replacing the fictional EIRP antenna with a microstrip patch antenna, the percentage of covered users drops for both optimization strategies. This is because users who have a higher horizontal distance between themselves and the UABS, experience a higher attenuation. Also, when a microstrip patch antenna is positioned higher, the range of the antenna increases since the angle between the user and the UABSs main lob decreases. The user will therefore experience less attenuation.

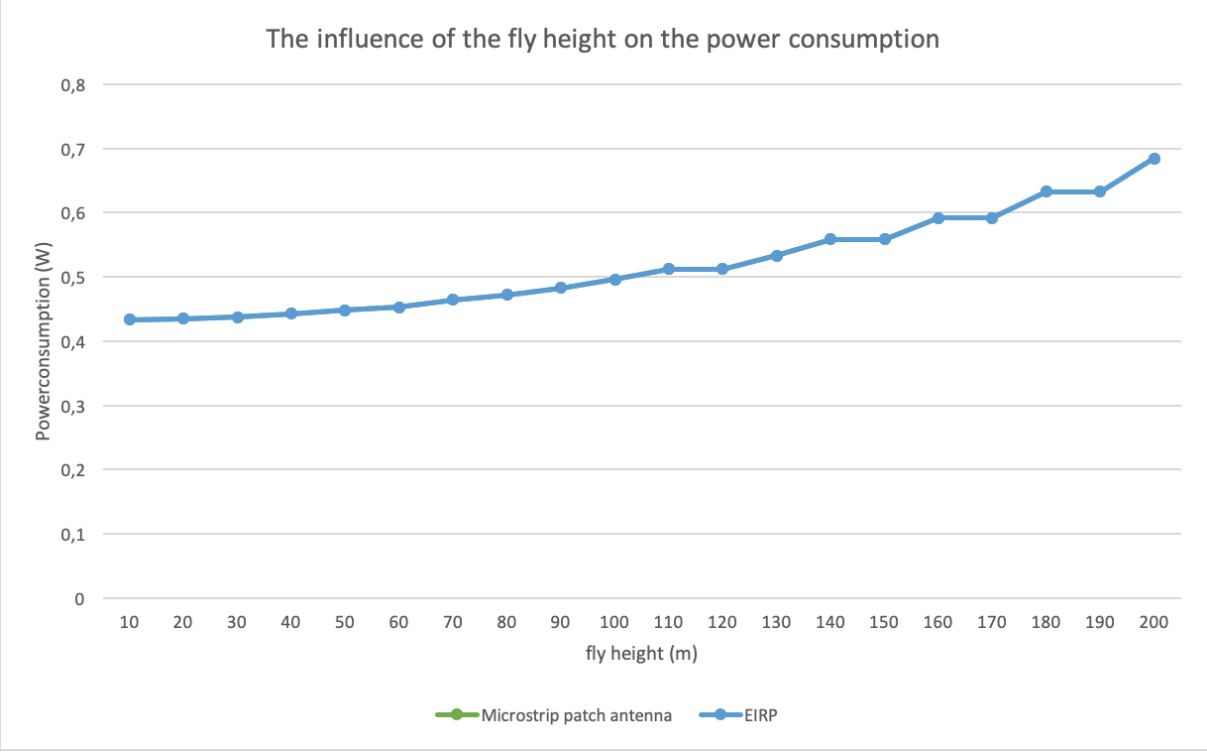

Figure 5.6: General design of a microstrip antenna

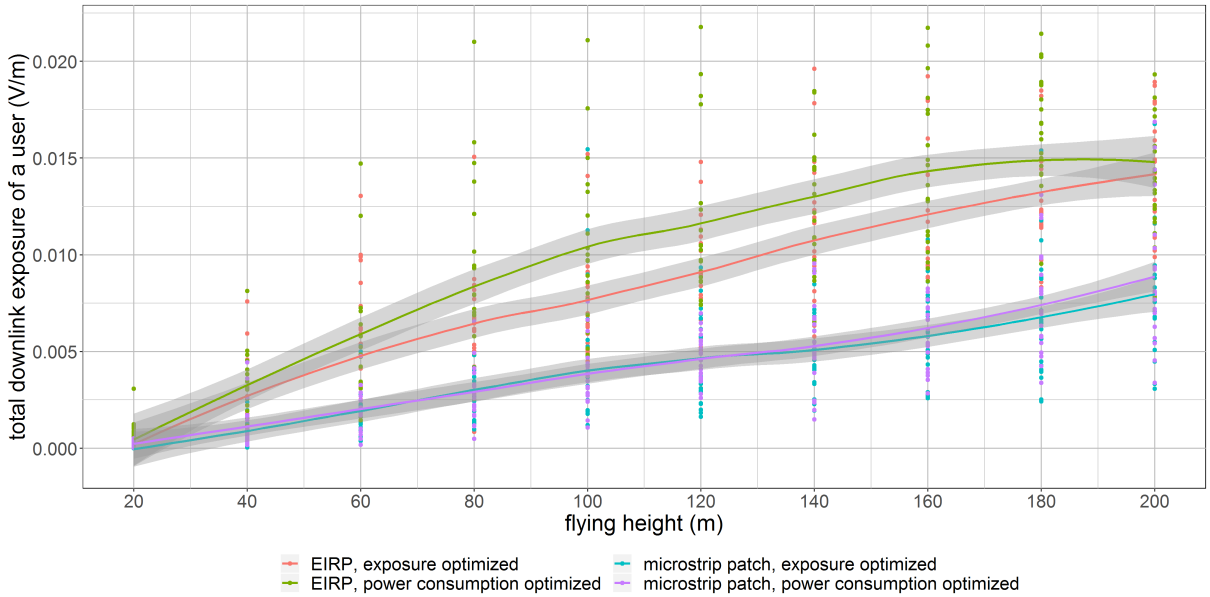

Figure 5.7: The influence of the flying height on the weighted average downlink exposure of users in the network.

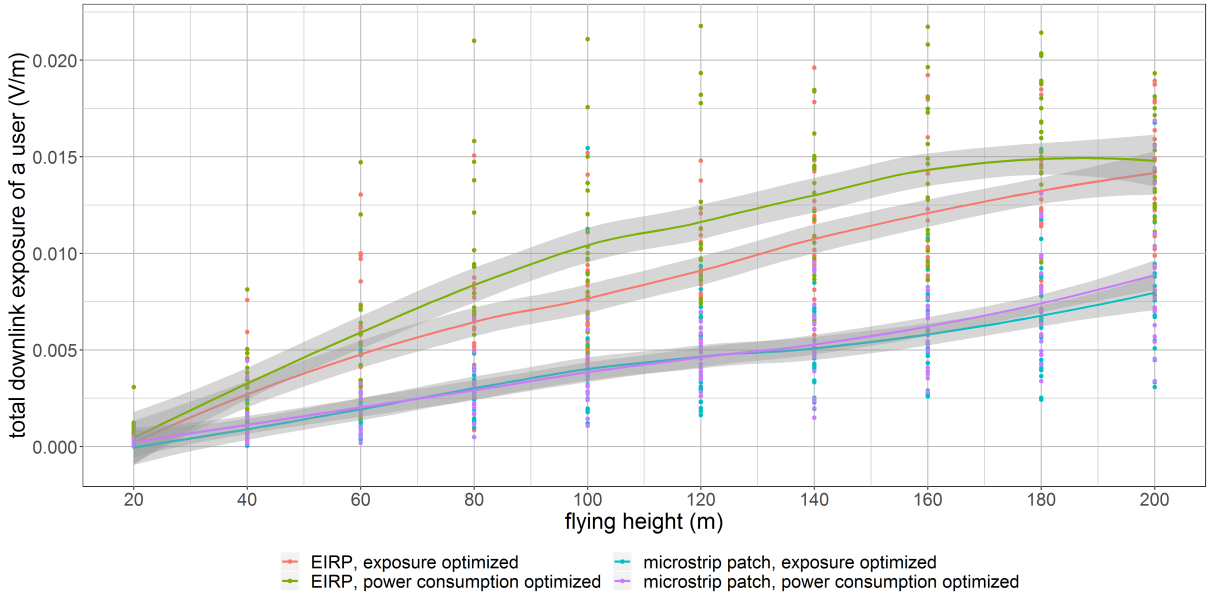

Figure 5.8: The influence of the flying height on the total power consumption of the network.

It becomes also clear that this advantage is limited. For a scenario of 224 users and one drone, the user coverage won't increase significantly anymore around an altitude of 120m.

Chart 5.10 shows the whole body SAR10g, deducted from all electromagnetic sources. This being exposure of all UABSs, the uplink exposure from the user's own device and the exposure of the devices from all other users. Thereafter, the weighted average of all whole body SAR10g

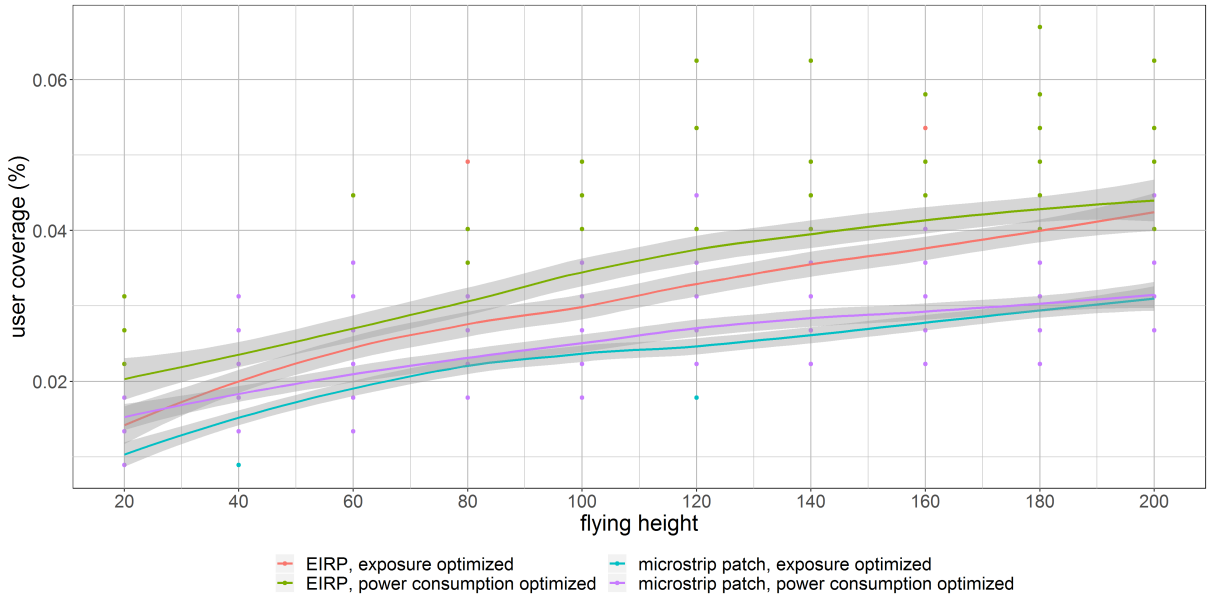

Figure 5.9: This graph shows the percentage of covered users by one drone for different flying heights.

values in the network is calculated with the 50th and 95th percentile being the most important values. This is because not only the mean values are important but also users who experience higher levels of whole body SAR10g.

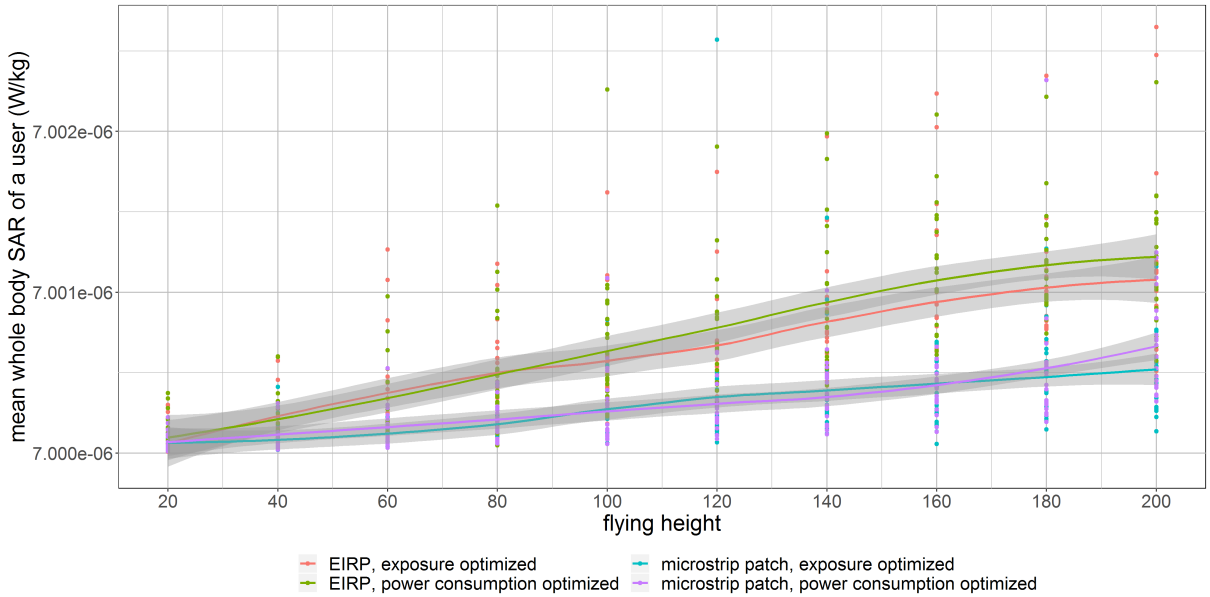

Figure 5.10: The influence of the flying height on the weighted average SAR_{10g} of users in the network.

5.3.2 Influence of the number of users

5.4 Scenario 3:

5.4.1 Influence of the flight altitude

This scenario examines the same cases as scenario 2 but there is no restriction on the number of UABSs. Unlike in scenario 2, fig. 5.11 and 5.14 show a clearer view on how the decision algorithms works. Antennae in an exposure optimized network cause less downlink exposure (fig. 5.11). On the other hand, a network generated for optimal power consumption requires indeed less energy as proven in figure 5.14.

Figure 5.11 shows how an equivalent isotropic radiator in and power consumption optimized network has the highest exposure when the UABS is close to the ground. An power consumption optimized network results in less number of drones which can also be seen on figure **??**. The network is still trying to cover as much users as possible as visible on figure 5.13 (with in this case less resources). Low flying drones need to account for increased pathloss by obstructing buildings. When the flying altitude increases, there is less pathloss and the electromagnetic exposure stabilizes. The same is applicable when replacing the equivalent isotropic radiator with a microstrip patch antenna but users will experience less electromagnetic radiation because of antenna aperture. Because the algorithm still tries to cover as much users as possible, the tool will react to this by introducing more drones (fig **??**).

When changing the optimization strategy towards an exposure optimized network, the lowest possible electromagnetic radiation is recorded with low flying drones at 20 m height with microstrip patch antennae. Using an equivalent isotropic radiator automatically increases electromagnetic radiation because of the absence of attenuation. This behavior results in an higher necessity of antenna carriers **??**.

Both **??** and 5.14 show that the network profit from increasing the flying altitude. Not only less drones are needed but also the power consumption is lower. Both can be explained by the lower pathloss when UABSs fly higher. If a user cannot be covered because an UABSs is too far away or is saturated with other users, the tool can simply add another UABS. The only remaining reason that a user can't be covered is because the position of the drone is obstructed by a building. The higher drones fly, the less change the position is obstructed by a building. In gent is this chance is zero when flying higher then 119 meters. Since the 'Artevelde Tower' is the highest building in Ghent.

Scenario 1 already proved that with low flying drones, the main source of electromagnetic radiation are UABS. This changes around 80 meters where UL electromagnetic radiation of the UE exceeds DL radiation in order to still be able to reach the high flying UABSs.

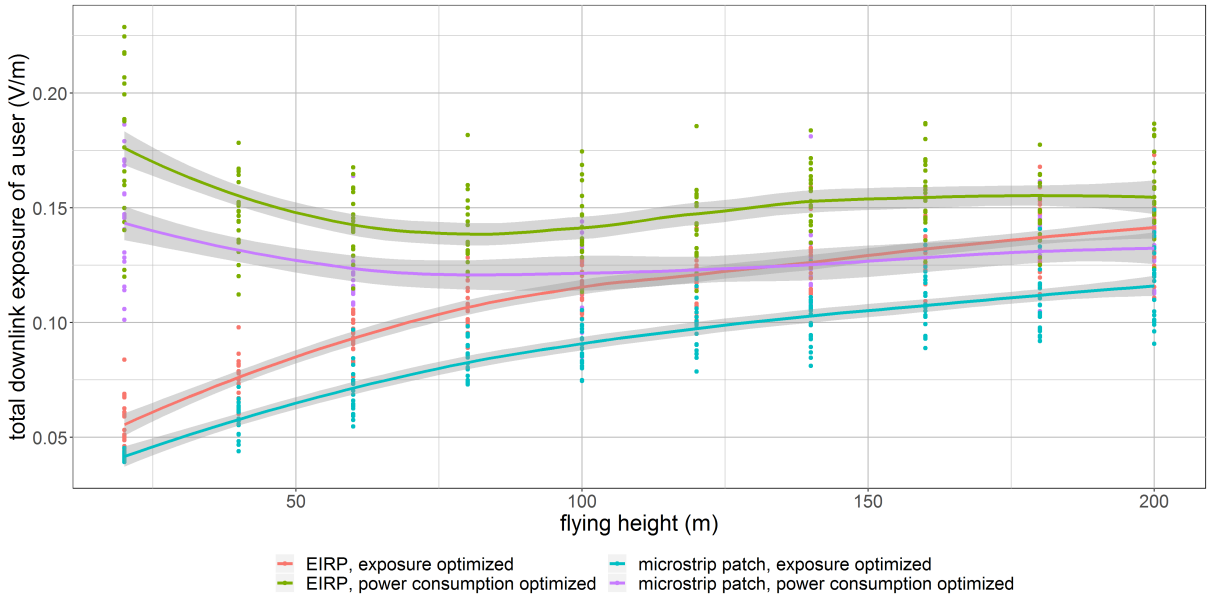

Figure 5.11: The influence of the flying height on the downlink electromagnetic radiation of the average user.

5.4.2 Influence of the number of users

todo

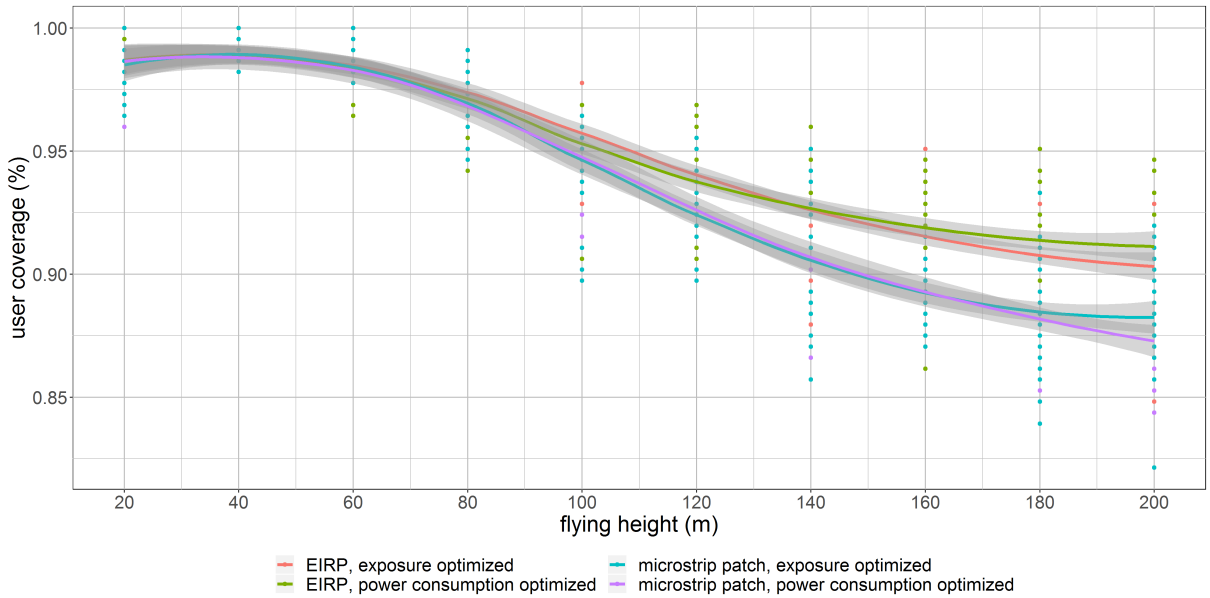

Figure 5.12: This graph shows the percentage of covered users by one drone for different flying heights.

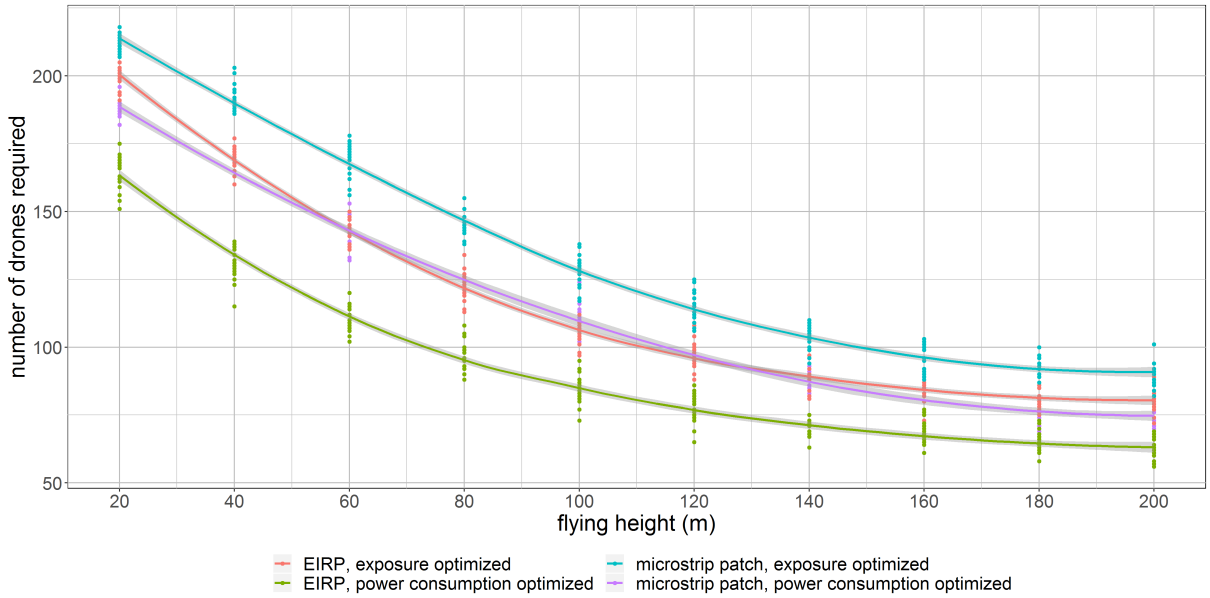

Figure 5.13: This graph shows how much drones are required for different flying heights while trying to achieve a 100% coverage.

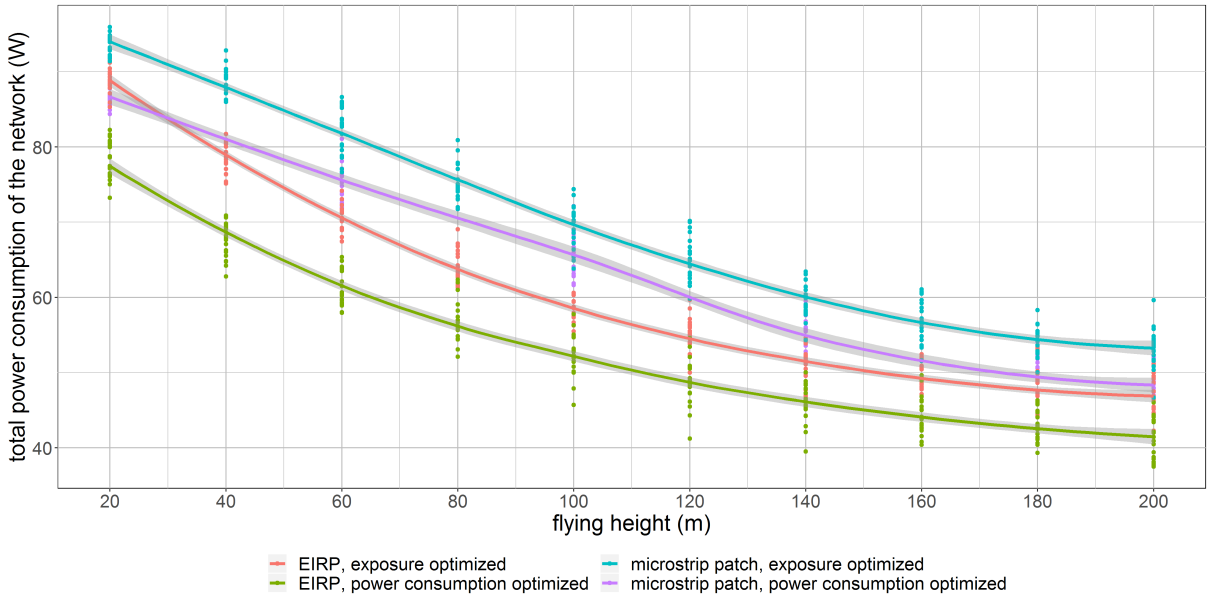

Figure 5.14: The influence of the flying height on the total power consumption of the network.

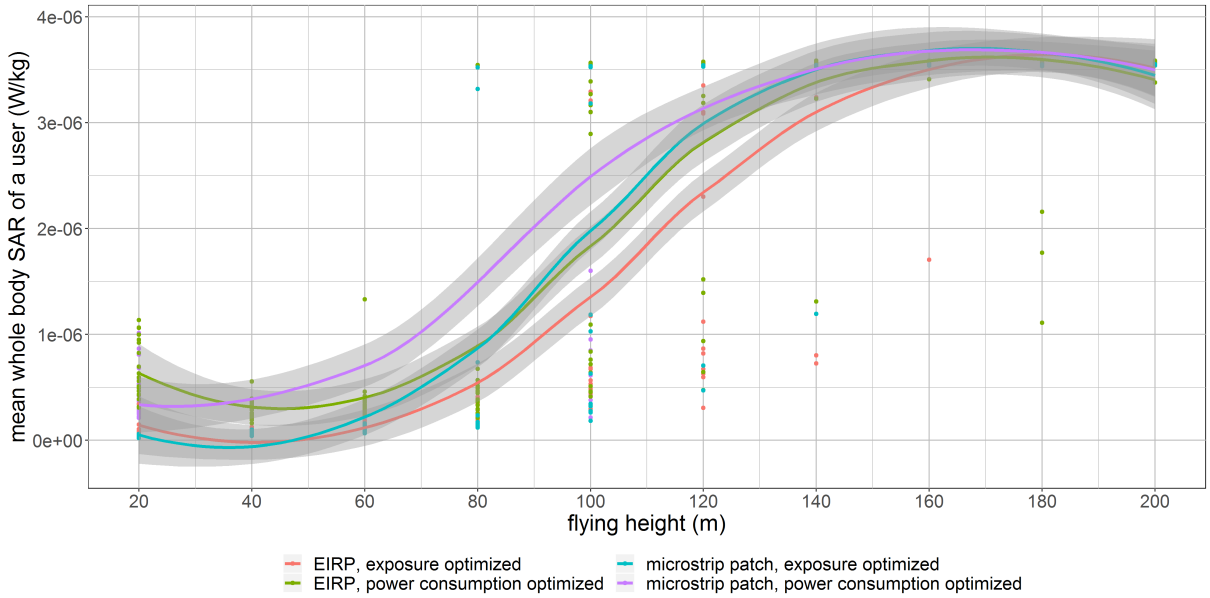

Figure 5.15: The influence of the flying height on the weighted average SAR_{10g} of users in the network.

6

Conclusions

todo

Bibliography

[1] *5G Wireless Systems Simulation and Evaluation Techniques*. Springer.

[2] D. standaard, "Base overschreed stralingsnormen na aanslagen," *De standaard*, 2016.

[3] L. Hardell and C. Sage, "Biological effects from electromagnetic field exposure and public exposure standards," *Biomedicine and Pharmacotherapy*, vol. 62, no. 2, pp. 104 – 109, 2008.

[4] "Electromagnetic fields (emf)," Nov.

[5] "kaart van mobiel netwerkbereik." `https://www.test-aankoop.be/hightech/gsms-en-smartphones/module/kaart-van-mobiel-netwerkbereik`. Accessed: 03-03-2020.

[6] M. Deruyck, J. Wyckmans, W. Joseph, and L. Martens, "Designing uav-aided emergency networks for large-scale disaster scenarios," *EURASIP Journal on Wireless Communications and Networking*, vol. 2018, 12 2018.

[7] v. v. d. v. e. l. Federale overheidsdienst: volksgezondheid, "Elektromagnetische velden en gezondheid: Uw wegwijzer in het elektromagnetische landschap," vol. 5, 2014.

[8] "Normen zendantennes." `https://omgeving.vlaanderen.be/normen-zendantennes`. Accessed: 14-10-2019.

[9] I. Guideline, "Guidelines for limiting exposure to time-varying electric, magnetic, and electromagnetic fields (up to 300 ghz)," *Health phys*, vol. 74, no. 4, pp. 494–522, 1998.

[10] D. Plets, W. Joseph, K. Vanhecke, and L. Martens, "Exposure optimization in indoor wireless networks by heuristic network planning," *Progress In Electromagnetics Research*, vol. 139, pp. 445–478, 01 2013.

[11] M. Deruyck, E. Tanghe, D. Plets, L. Martens, and W. Joseph, "Optimizing lte wireless access networks towards power consumption and electromagnetic exposure of human beings," *Computer Networks*, vol. 94, 12 2015.

[12] D. Plets, W. Joseph, S. Aerts, K. Vanhecke, G. Vermeeren, and L. Martens, "Prediction and comparison of downlink electric-field and uplink localised sar values for realistic indoor wireless planning," *Radiation Protection Dosimetry*, vol. 162, no. 4, pp. 487–498, 2014.

[13] D. Plets, W. Joseph, K. Vanhecke, and L. Martens, "Downlink electric-field and uplink sar prediction algorithm in indoor wireless network planner," in *The 8th European Conference on Antennas and Propagation (EuCAP 2014)*, pp. 2457–2461, IEEE, 2014.

[14] S. Kuehn, S. Pfeifer, B. Kochali, and N. Kuster, "Modelling of total exposure in hypothetical 5g mobile networks for varied topologies and user scenarios," *Final Report of Project CRR-816, Available on line at: https://tinyurl. com/r6z2gqn*, 2019.

[15] D. Plets, W. Joseph, K. Vanhecke, G. Vermeeren, J. Wiart, S. Aerts, N. Varsier, and L. Martens, "Joint minimization of uplink and downlink whole-body exposure dose in indoor wireless networks," *BioMed research international*, vol. 2015, 2015.

[16] I. Singh and V. Tripathi, "Micro strip patch antenna and its applications: a survey," *Int. J. Comp. Tech. Appl*, vol. 2, no. 5, pp. 1595–1599, 2011.

[17] K. Kashwan, V. Rajeshkumar, T. Gunasekaran, and K. S. Kumar, "Design and characterization of pin fed microstrip patch antennae," in *2011 Eighth International Conference on Fuzzy Systems and Knowledge Discovery (FSKD)*, vol. 4, pp. 2258–2262, IEEE, 2011.

[18] I. Singh and V. Tripathi, "Micro strip patch antenna and its applications: a survey," *Int. J. Comp. Tech. Appl*, vol. 2, no. 5, pp. 1595–1599, 2011.

[19] A. Sudarsan and A. Prabhu, "Design and development of microstrip patch antenna," *International Journal of Antennas (JANT) Vol*, vol. 3, 2017.

[20] P. Joshi, D. Colombi, B. Thors, L.-E. Larsson, and C. Törnevik, "Output power levels of 4g user equipment and implications on realistic rf emf exposure assessments," *IEEE Access*, vol. 5, pp. 4545–4550, 2017.

[21] "Bundesamt für strahlenschutz." `http://www.bfs.de/SiteGlobals/Forms/Suche/BfS/EN/SARsuche_Formular.html`. Accessed: 14-10-2019.

[22] A. Gati, E. Conil, M.-F. Wong, and J. Wiart, "Duality between uplink local and downlink whole-body exposures in operating networks," *IEEE transactions on electromagnetic compatibility*, vol. 52, no. 4, pp. 829–836, 2010.

Appendices

A

Radiation patterns: datasheet

Table A.1 gives an overview of the attenuation in the E and H plane. The first radiation pattern is with a square groundplane with an edge of 0.060 meter while the second pattern is more of a rectangular shape with a width of 0.0524m and a lenght of 0.0438m. All other settings are equal as defined in 4.2.4

Table A.1: Overview of attenuation in dBm

	pattern 1		pattern 2	
angle	E	H	E	H
0	0,00	0,00	0	0
10	-0,17	-0,14	-0.1561	-0.158
20	-0,67	-0,57	-0.5797	-0.6257
30	-1,48	-1,27	-1.263	-1.386
40	-2,57	-2,22	-2.193	-2.412
50	-3,90	-3,39	-3.357	-3.665
60	-5,40	-4,73	-4.741	-5.099
70	-7,09	-6,23	-6.337	-6.658
80	-8,82	-7,87	-8.136	-8.278
90	-10,54	-9,70	-10.11	-9.88
100	-12,20	-11,84	-12.14	-11.34
110	-13,73	-14,37	-13.81	-12.47
120	-15,04	-17,65	-14.42	-13.00
130	-16,01	-21,83	-13.72	-12.82
140	-16,47	-23,63	-12.41	-12.08
150	-16,42	-20,37	-11.15	-11.15
160	-16,05	-17,49	-10.21	-10.33
170	-15,69	-15,93	-9.683	-9.786
180	-15,54	-15,54	-9.596	-9.596
190	-15,69	-16,30	-9.963	-9.784
200	-16,05	-18,44	-10.79	-10.33
210	-16,42	-22,85	-12.07	-11.15
220	-16,47	-31,23	-13.71	-12.07
230	-16,00	-24,07	-15.25	-12.80
240	-15,03	-18,05	-15.65	-12.99
250	-13,72	-14,42	-14.3	-12.45
260	-12,20	-11,81	-12.11	-11.33
270	-10,54	-9,70	-9.882	-9.866
280	-8,82	-7,87	-7.859	-8.267
290	-7,09	-6,23	-6.069	-6.649
300	-5,40	-4,73	-4.502	-5.093
310	-3,90	-3,39	-3.154	-3.661
320	-2,57	-2,22	-2.029	-2.409
330	-1,48	-1,27	-1.138	-1.384
340	-0,67	-0,57	-0.4963	-0.6246
350	-0,17	-0,14	-1143	-0.1575

B

Radiation patterns: example configuration

In listing 2 is a possible configuration described for a radiation pattern. It is important to notice that this example configuration does not represent the used configuration in this master dissertation. The `radiatoinPattern`-tag consist of a `slices`-tag. This tag can contain as much slices as desired. In this example, 3 slices are defined indicated with the `attenuation`-tag. This tag contains a mandatory attribute `az` which defines the azimuth angle to which all underlying attenuation values belong. Inside the `attenuation`-tag are all attenuation values written in a `value`-tag.

The tool distributes all values equally over the 180° of that slice. In the example below, each `attenuation`-tag contains 10 values meaning that the exact attenuation is known every 20°.

The highlighted value of -14,42 is therefore measured at an azimuth angle of 0° and an elevation angle of 120° (counterclockwise).

```
<radiationPattern>
    <slices>
        <attenuation az="0">
            <value>0</value>
            <value>-0.5797</value>
            <value>-2.193</value>
            <value>-4.741</value>
            <value>-8.136</value>
            <value>-12.14</value>
            <value>-14.42</value>
            <value>-12.41</value>
            <value>-10.21</value>
            <value>-9.596</value>
        </attenuation>
        <attenuation az="90">
            <value>0</value>
            <value>-0.6257</value>
            <value>-2.412</value>
            <value>-5.099</value>
            <value>-8.278</value>
            <value>-11.34</value>
            <value>-13.00</value>
            <value>-12.08</value>
            <value>-10.33</value>
            <value>-9.596</value>
        </attenuation>
        <attenuation az="180">
            <value>0</value>
            <value>-0.4963</value>
            <value>-2.029</value>
            <value>-4.502</value>
            <value>-7.859</value>
            <value>-12.11</value>
            <value>-15.65</value>
            <value>-13.71</value>
            <value>-10.79</value>
            <value>-9.596</value>
        </attenuation>
    </slices>
</radiationPattern>
```

Listing 2: Example configuration of a radiation pattern.